Thesis for the Degree of Doctor of Philosophy

Promotive effect of spirulina proteins on skin wound healing

by

Ping Liu

Department of Food and Life Science

The Graduate School

Pukyong National University

August 2019

Promotive effect of spirulina proteins on skin wound healing

(스피루리나 단백질의 피부 상처 치유 촉진 효과)

Advisor: Prof. Taek-Jeong Nam

by

Ping Liu

A thesis submitted in partial fulfillment of the requirements
for the degree of

Doctor of Philosophy

in Department of Food and Life Science, The Graduate School, Pukyong National University

August 2019

Promotive effect of spirulina proteins on skin wound healing

A dissertation

by

Ping Liu

Approved by:

(Chairman) Jae-Sue Choi

(Member) Sang-Gil Lee

(Member) In-Soo Kong

(Member) Youn-Hee Choi

(Member) Taek-Jeong Nam

August 24, 2019

CONTENTS

LIST OF TABLES

LIST OF FIGURES

ABBREVIATIONS

4EBP1	eukaryotic translation initiation factor 4E (eIF4E) -binding protein 1
Akt	serine-threonine kinase
α-SMA	Alpha-smooth muscle actin
BCA	Bicinchoninic acid
β-ME	β-Mercaptoethanol
BPB	bromophenol blue
BrdU	Bromodeoxyuridine
BSA	bovine serum albumin
CAT	catalase
CDK2	cyclin-dependent kinase 2
CDK4	cyclin-dependent kinase 4
CDK6	cyclin-dependent kinase 6
CO_2	carbon dioxide
COL1A1	collagen type I alpha 1
COL1A2	collagen type I alpha 2
CRD	cysteine-rich domain
DMEM	Dulbecco's Modified Eagle Medium
DTT	dithiothreitol
ECM	extracellular matrix
EGF	epidermal growth factor
EGFR	epidermal growth factor receptor
eIF4E	eukaryotic translation initiation factor 4E
ELISA	enzyme-linked immunosorbent assay

ERK	extracellular signal-regulated kinase
FBS	fetal bovine serum
GDP	guanosine diphosphate
Grb2	growth factor receptor binding protein 2
GSK3β	glycogen synthase kinase 3 beta
GTP	guanosine-5'-triphosphate
H_2SO_4	sulfuric acid
HRP	horseradish peroxidase
IgG	anti-rabbit Immunoglobulin G
MAPK	mitogen-activated protein kinase
MDA	lipid peroxidation
MEK	mitogen-activated protein kinase kinase
MMP	matrix metalloproteinase
mTOR	mammalian target of rapamycin
MTS	3-(4,5-dimethylthiazol-2-yl)-5-(3-caboxymethoxy-phenyl)-2-(4-sulfonyl)-2H-terazolium
NF-κB	nuclear factor kappa-light-chain-enhancer of activated B cells
O^{2-}	superoxide anion free radicals
p70S6K	p70 ribosomal protein S6 kinase
PAK	p21-activated kinase
PBS	phosphate-buffered saline
PDK1	3-phosphoinositide-dependent protein kinase-1
PDK2	3-phosphoinositide-dependent protein kinase-2
PI	propidium iodide
PI3K	phosphoinositide 3-kinase

PIP	procollagen type I C-peptide
PIP2	phosphatidylinositol-4,5-bisphosphate
PIP3	phosphatidylinositol-3,4,5-triphosphate
PKC	protein kinase C
PMSF	phenylmethylsulfonyl fluoride
pRb	retinoblastoma protein
PTEN	phosphatase and tensin homolog
PVDF	polyvinylidene difluoride
Q-TOF MS/MS	quadrupole time of flight mass spectrometry
RBD	Ras-binding domain
RIPA	radioimmunoprecipitation
ROS	reactive oxygen species
RTK	receptor tyrosine kinase
SDS	sodium dodecyl sulfate
SDS-PAGE	sodium dodecyl sulfate polyacrylamide gel electrophoresis
Ser	serine
SFM	serum-free medium
SH2	Src homology domain 2
SOD	superoxide dismutase
SOS	Son of Sevenless
TBA	thiobarbituric acid
TBS-T	tris-buffered saline with 0.1% tween 20
TGF-β	transforming growth factor-β
Thr	threonine
TNF	tumor necrosis factor

Tris-HCl	Tris- hydrochloride
Tyr	tyrosine

Promotive effect of spirulina proteins on skin wound healing

Ping Liu

부경대학교 대학원 식품생명과학과

요 약

피부는 표피와 진피로 구성되며, 인체의 외부환경에 대한 가장 큰 방어기관으로 작용한다. 따라서 피부의 상처는 내과 신체의 경계를 허물어 심한 육체적인 부담을 초래한다. 상처의 치유 과정에 관여하는 주요 복구세포로 섬유 아세포가 있으며, 피부 상처 치유를 위해 섬유 아세포에 관한 연구가 필요하다. 청녹색의 미세조류인spirulina는, 높은 단백질 함량 및 영양가로 이상적인 영양공급원으로 이용되어 왔으며, 현재 spirulina가 가지고 있는 영양소 성분이 여러 질병(항암, 노화 억제, 비특이적 세포 면역 기능 강화)을 효과적으로 치료하는 것으로 광범위하게 연구되고 있다. 최근연구에 의하면 *Spirulina platensis*의 추출물은 섬유 아세포의 증식을 촉진하고 상처치료를 촉진하는 것으로 밝혀졌지만 아직까지 상처치료 작용에 의한 메커니즘은 완전히 이해되지 않았다. 따라서 본 연구에서는 인간 피부 섬유 아세포인 CCD-986sk와 C57BL-6 마우스에 대한 spirulina 조단백질(SPCP)의 효과와 해당 메커니즘을 규명하고자 하였다.

먼저 *in vitro* 분석을 위해 인간 피부 섬유 아세포 세포주인 CCD-986sk 세포가 인간 피부 세포에 대한 스피룰리나 조단백질 (SPCP)의 효과를 측정하기 위해 사용되었다. CCD-986sk 세포의 증식에 대한 SPCP의 효과를 확인하기 위한 Bromodeoxyuridine (BrdU) assay와 MTS assay 분석을 통해 SPCP가 CCD-986sk 세포의 증식을 촉진한다는 것을 확인하였다. 다음으로 피부상처 치유에 주요 역할을 하는 콜라겐과 elastase를 효소 결합 면역 흡착 분석 (ELISA)을 하였을 때, SPCP를 처리 한 세포에서 콜라겐 형성이 용량 의존적으로 개선되는 것을 보여 주었으며, elastase 활성은 감소했다. 또한 섬유 아세포의 새로운 조직 형성에 증식 및 이동과정을 동반하는것으로 밝혀졌다. 따라서 CCD-986sk 세포의 이동에 대한 SPCP의 효과를 wound-healing assay로 분석하였을 때, SPCP가 CCD-986sk 세포의 이동을 유의하게 유도하는 것을 확인하였다.

세포 증식은 세포주기와 성장인자 신호전달 경로사이의 상호작용에 의해 조절된다. 따라서, 세포주기 분석을 시행하였을 때, SPCP는 CCD-986sk 세포의 G_0/G_1 상으로부터 S 및 G_2/M 상으로 진행하는 것을 촉진 하였다. 또한, 세포주기 관련 단백질의 발현 수준을 western blot 분석을 하였을 때, SPCP가 cyclin D1, cyclin E, Cyclin-dependent kinase 2 (CDK2), Cyclin-dependent kinase 4 (CDK4) 및 Cyclin-dependent kinase 6 (CDK6)의 발현을 유의하게 증가시키고 CDK 억제제인 p21과 p27의 발현을 억제하는 것을 확인하였다 다음으로 주요 세포 성장 신호 전달 경로를 western blot 분석하였을 때, SPCP는 CCD-986sk 세포에서 상피 세포 성장 인자 수용체 (EGFR) 활성을 상향 조절하였으며, EGFR의 신호를 마이토겐-활성화 단백질 키나아제 (MAPK) 경로로 전달하는 GRB2, SHC 및 구아닌 뉴클레오타이드 교환 단백질 (SOS)를 포함한 EGFR의 어댑터 단백질의 발현의 증가 및 MAPK/세포 외 신호 조절 키나아제 (ERK) 신호 전달 경로의 활성화를 확인하였다. 다음으로 SPCP는 또다른 세포성장 신호전달경로인 phosphoinositide 3-kinase (PI3K)와 serine-threonine kinase (Akt)의 인산화와 활성화를 촉진한다는 것을 확인하였다. PI3K/Akt 신호 전달 경로의 억제제인 PTEN을 분석하였을 때, PTEN의 발현 수준이 SPCP 처리에 의해 감소하였으며, 포유류 세포 증식 조절에 중요한 역할을하며 p-Akt에 의해 활성화되는 mTOR 의 인산화가 증가로 mTOR신호가 활성화되는 것을 확인하였다. mTOR 신호에 대한 중요한 인산화 기질인 4EBP1 및 p70S6K 의 인산화 SPCP에 의해 촉진되었으며, 핵에서 eIF4E의 발현증가로 SPCP에 의해 활성화된 4EBP1이 eIF4E를 방출하여 단백질 합성을 촉진하는 것을 확인하였다. 많은 전사 인자의 활성은 β-catenin의 영향을 받으며, GSK3β에 의해 분해 될 수 있다. Western blot 분석은 GSK3β의 활성이 p-Akt에 의해 억제되었으며, β-catenin이 방출되었다. CCD-986sk 세포에서 SPCP에 의한 증식 및 이동에서 ERK 및 Akt 신호전달경로의 역할을 추가로 확인하기 위해 ERK 억제제 (U0126) 및 PI3K 억제제 (LY294002)를 사용하였다. 그 결과, CCD-986sk 세포에서의 SPCP 유도 된 증식 및 이동은 U0126 및 LY294002에 의해 차단되었으며, 이러한 결과로 SPCP에 의해 유도 된 증식 및 이동이 ERK 및 Akt 신호 전달 경로에 의해 조절된다는 것을 확인하였다. 따라서 본 연구 결과는 SPCP가 인간 섬유 아세포 CCD-986sk 세포의 증식과 이동을 촉진시키고, 이 과정에서 EGFR/MAPK 및 PI3K/Akt 신호 전달 경로가 주요 역할을하는 것을 의미한다.

In vitro 실험에서의 결과를 토대로 *in vivo* 모델에 적용하여 그 효과를 밝히기 위해 피부상처를 가진 mouse 모델을 사용하여 SPCP의 상처치유촉진효과를 검증하였다. 특히, SPCP는 피부상처를 가진 마우스 모델에서 상처 치유를 촉진하였으며, SPCP의 처리는 바세린을 처리하였을 때보다 상처봉합율이 높은 것을 확인하였다. 또한 산화 스트레스는 상처 치유를 지연시키는 것으로 잘 알려져 있기 때문에 상처 치유에 대한 SPCP의 항산화 효과를 분석하였다. ELISA의 결과는 SPCP가 superoxide dismutase (SOD)와 catalase (CAT)의 활성을 증가 시킨다는 것을 의미하였으

며, 지질 과산화 (MDA)의 수준은 SPCP의 처리에 의해 감소되었다. 이러한 결과는 SPCP가 C57BL/6 마우스의 피부 상처 치유에 항산화 효과가 있음을 나타낸다. 또한, SPCP는 C57BL / 6 마우스의 피부 창상 조직에서 α 평활근 액틴 (α-SMA)의 발현을 촉진시켰으며, 이 결과는 SPCP가 근섬유 아세포의 분화를 촉진한다는 것을 시사한다. 한편, western blot 결과는 마우스 피부 창상 조직에서 SPCP에 의해 ERK와 Akt의 인산화가 유의하게 향상되었으며, SPCP가 ERK 및 Akt 신호 전달 경로에 의해 세포 증식을 촉진한다는 것을 의미한다. 다음으로 변형 성장 인자 -β1 (TGF-β1)/Smad2 신호 전달 경로가 SPCP에 의해 활성화되었으며, 콜라겐 I 형 알파 1 (COL1A1)과 콜라겐 I 형 알파 2 (COL1A2)의 발현 또한 촉진시켰다. 이 결과는 SPCP가 상처 치료에서 콜라겐의 축적을 유도 함을 나타냅니다.

종합하면, SPCP가 항산화제에 의해 피부 상처 치유를 촉진시키고 피부 섬유 아세포의 증식과 이동을 증가시키고 콜라겐 합성을 촉진하여 근섬유 아세포 수준을 증가시킴을 확인하였다. 따라서 이러한 결과는 SPCP가 피부 창상 치유를 촉진하는 분자 메커니즘을 밝혀주고 피부 상처 치료를위한 잠재적인 치료제로서 활용될 수 있음을 시사한다.

I. INTRODUCTION

1. Spirulina

There are many kinds of microalgae. And the microalgae cells contain high-value nutrients, such as proteins, lipids, algal polysaccharides, β-carotene, and various inorganic elements (such as Cu, Fe, Se, Mn, Zn, etc.) (Buono *et al.*, 2014; Raposo and Rui, 2013). The microalgae have a high content of carotenoid and the functions of coloring and nutrition. It can be used to prevent cancer, resist radiation, delay aging, and enhance the body's immunity (Kubatka *et al.*, 2015; Sheih *et al.*, 2010). Microalgae cells have high glycerin content and are high-quality cosmetic raw materials (Bilal *et al.*, 2017; Raposo and Rui, 2013). They are also widely used as organic intermediates in the chemical, light industry and pharmaceutical industries (Spolaore *et al*., 2006; Wu *et al*., 2016).

Spirulina belongs to the genus Cyanophyta, Oscilatoriales, and Oscilatoriaceae. The spirulina, which is widely produced, two varieties, including the blunt apex *Spirulina platensis* (*S. platensis*) and *Spirulina maxima* (*S. maxima*) (Saranraj, 2014). Spirulina is widely distributed in oceans and lakes and usually floats in low- and medium-tidal seawater or attaches on other algae and appendages (Saranraj, 2014). Naturally grown spirulina is mainly distributed in a different environment, including soil, marshes, sand, seawater, and freshwater (Saranraj, 2014). Spirulina is rich in amino acids and trace elements, including many essential amino acids that the human body cannot synthesize (Lee *et al.*, 2017). Meanwhile, spirulina is also rich in polysaccharides and more than ten vitamins and rich in minerals and biologically active substances (Wang and Zhang, 2016; Wu *et al.*, 2016).

Studies have shown that spirulina and its extracts have the effects of preventing and inhibiting cancer, immune promotion, antibacterial activity, antioxidant activity and antihypertensive activity (Heussner *et al.*, 2012; Kepekçi *et al.*, 2013; Kim *et al.*, 2010; Wu *et al.*, 2016). It was reported that spirulina can protect stem cells from LPS-induced proliferation decline (Bachstetter *et al.*, 2010). C-phycocyanin which was extracted from spirulina promoted the migration of cells in the dermal wound healing (Madhyastha *et al.*, 2012). These reports indicated that spirulina may have the potential of promoting skin wound healing. This study was aimed to determine the effect of spirulina crude protein (SPCP) on the wound healing and further explore the mechanisms of SPCP in wound healing.

2. The skin

The skin is the largest organ in the body and is a protective barrier against the various external invasions (Sorg *et al.*, 2017). The composition of the skin is complex and orderly, consisting of epidermis, dermis and skin-accessory organs (Yannas *et al.*, 2017). Normal and intact skin protects the body from external substances and microorganisms, regulates body temperature, and prevents tissue dehydration (Makoto *et al.*, 2015). Damage to the skin tissue not only causes damage to the subcutaneous tissue but also affects the internal balance of the body. There are many causes of skin damage in daily life, such as friction, sharp cuts, burns, etc. When the skin tissue is damaged, the body initiates the wound healing process (Abood *et al.*, 2014). If the acute skin damage is not properly repaired, a chronic, unhealed wound or a hypertrophic scar tissue is formed (Zhong *et al.*, 2010). Therefore, it is very necessary to find a way to promote wound healing.

3. Wound healing

The healing process after skin damage is a very complex process. After skin trauma, various cytokines first recruit macrophages, neutrophils, and other repair-related cells, and then act on fibroblasts, keratinocytes and so on (Hu *et al.*, 2016). In tissue repair, fibroblasts are the main repair cells in the healing process, and their biological functions play a vital role in wound healing (Chiquet *et al.*, 2015; Darby *et al.*, 2014). It was shown that fibroblasts are engineer, administrator, and builder of wound healing (Singer and Clark, 1999). Moreover, fibroblasts are the main repairing cells for the formation of granulation tissue, synthetic collagen, and extracellular matrix during wound healing (Kim *et al.*, 2007). At the same time, autocrine growth factors can also regulate the wound healing process (Barrientos *et al.*, 2008). Therefore, changes in the function of fibroblasts play a pivotal role in wound healing. During the whole process of wound healing, fibroblasts mainly exhibit two different biological functions. The first one is proliferation and migration characteristics and the second one is a secretory function. These two characteristics are interdependent (Gonzalez *et al.*, 2016; Werner *et al.*, 2007). Studies have shown that abnormal fibroblast proliferation may be one of the important factors in the difficult healing of skin lesions (Darby and Hewitson, 2007).

Studies have found that myofibroblasts also play a role in wound healing. Although it is a fibroblast, it has the characteristics of both fibroblasts and smooth muscle cells (Gabbiani, 2003). Myofibroblasts differentiate from fibroblasts. Myofibroblasts are involved in wound healing and collagen secretion in the late stage of tissue repair (Desmoulière, 1995). The differentiation of myofibroblasts is closely related to the quality and speed of wound healing (Jester *et al.*, 1999). It was found that when a wound occurs, fibroblasts first migrate to the wound site, producing a

wound contraction effect (Li and Wang, 2011). Cytokines and strain during contraction affect the differentiation of fibroblasts into myofibroblasts. Once the differentiation is successful, the actin skeletons in the fibroblasts are aligned in the direction of the tension and participate in the wound contraction process (Desmoulière *et al.*, 2005). It is concluded that fibroblast is one of the main cells for wound healing. It can regulate the process of wound healing by chemotaxis, proliferation, differentiation, and secretion (McAnulty, 2007).

4. Wound healing signaling pathway

Wound healing is an ordered dynamic process triggered by the interaction of many types of cells and molecules. Platelets, keratinocytes, immune surveillance cells, microvascular cells, and fibroblasts are critical in the process of tissue integrity recovery (Guo and DiPietro, 2010). Wound healing can be divided into four stages: coagulation, inflammatory response, granulation tissue formation (proliferation phase), remodeling or scar formation (Martin, 1997). The proliferation of cells is regulated by many signaling pathways (Hongxue *et al.*, 2015; Ling *et al.*, 2017; Liu *et al.*, 2017).

4.1. EGFR signaling pathway

Epidermal growth factor receptor (EGFR) is the most well-known cell proliferation protein in body tissues (Li *et al.*, 2015; Wei and Hui, 2002). EGFR is a transmembrane protein, which is divided into three parts: one end of the protein is located outside the cell, another part is located in the cell membrane andthe other end is located in the cell (Krasinskas, 2011). This allows EGFR receptors to bind to other extracellular proteins, called ligands, to help cells receive signals and respond

to their environment (Komposch and Sibilia, 2015). When EGFR binds to ligands, it attaches to another nearby EGFR receptor and forms a complex (dimer), thus entering an active state and activating intracellular signaling pathways (Jorissen *et al.*, 2003; Schreier *et al.*, 2014).

EGFR receptor protein is a member of the receptor tyrosine kinases (RTKs) family. It can activate two signaling pathways. They are Ras/Raf/mitogen-activated protein kinase kinase (MEK)/extracellular signal-regulated kinase (ERK) pathway involved in cell proliferation, and PI3K/Akt/mTOR pathway involved in cell survival (Li *et al.*, 2014; Rajaram *et al.*, 2017). Ras/Raf/MEK/ERK signaling pathway is responsible for controlling gene transcription activity and cell cycle (Chambard *et al.*, 2007; Zhang and Liu, 2002). And PI3K/Akt/mTOR signaling pathway can activate anti-apoptotic signal (Vara *et al.*, 2004). Therefore, EGFR receptor protein plays an important role in cell proliferation and survival.

4.1.1. Ras/Raf/MEK/ERK signaling pathway

The Ras/Raf/MEK/ERK signaling pathway can be activated by growth factors and mitogens, and then regulate the gene expression and cell proliferation. The pathway consists of a three-tiered kinase module, i.e. Raf, MEK and ERK kinase which are activated by phosphorylation in turn.

ERK is a kind of serine/threonine (Ser/Thr) protein kinase discovered in the late 1980s (Cruz and Cruz, 2007). ERK is a signal transduction protein that transmits mitogen signals (Martinez-Lopez and Singh, 2014). It is normally located in the cytoplasm and translocated to the nucleus after activation to regulate the activity of transcription factors and produce cellular effects (Sun *et al.*, 2015). Artificial cloning and sequencing analysis showed that there are two subtypes of

ERK, including ERK1 and ERK2 (Peng *et al.*, 2010). They are widely expressed and involved in regulating a series of physiological processes in different cells, including meiosis, mitosis, late mitosis and so on (Johnson and Lapadat, 2002). Many stimulators such as growth factors, cytokines, viruses, ligands of G protein-coupled receptors and oncogenes can activate this signaling pathway (Kolch, 2000; Wortzel and Seger, 2011).

Ras as the upstream protein of Raf/MEK/ERK signaling pathway, is the first discovered small G protein (Vojtek and Der, 1998). It is the product of gene *ras*. It has the binding conformation of activated Guanosine-5'-triphosphate (GTP) and inactivated guanosine diphosphate (GDP) (Kuriyama *et al.*, 1996). The two conformations can be transformed into each other and play a switching role in signal transduction (Young *et al.*, 2009). Ras is activated by many stimulants, such as epidermal growth factor (EGF) (Rozakis-Adcock *et al.*, 1993), tumor necrosis factor (TNF) (Takino *et al.*, 2014), protein kinase C (PKC) activator and members of Src family (Johnson, 2008). When extracellular signals bind to receptors, growth factor receptor binding protein 2 (Grb2), as a junction molecule, binds to activated receptors and interacts with a proline-rich sequence at the C-terminal of Son of Sevenless (SOS) to form a receptor-Grb2-SOS complex (Rojas *et al.*, 1996). The binding of SOS to Tyr phosphorylation sites on receptor or receptor substrate proteins leads to the translocation of SOS to the membrane (Margarit *et al.*, 2003), a high concentration of SOS was formed near Ras. The combination of SOS and Ras-GDP promotes GTP to replace GDP on Ras, transforms Ras from inactivation to activation, activates Ras and Ras pathway (Boriack-Sjodin *et al.*, 1998).

Raf is a Ser/Thr protein kinase. It has three types. They are Raf-1, A-Raf, and B-Raf (Hindley and Kolch, 2002; Zebisch and Troppmair, 2006). Raf-1 is the

most widely studied and functional kinase (Dhillon and Kolch, 2002). Ras, as an upstream activator protein, transfers Raf from the cytoplasm to the cell membrane by binding two regions of high affinity and Raf-1N-terminal (Ras-binding domain (RBD) and cysteine-rich domain (CRD)) (Cho *et al.*, 2012; Fetics *et al.*, 2015). However, the activation mechanism of Raf is still unclear, only related to the Ser/Thr phosphorylation of Raf (Dhillon and Kolch, 2002). Its phospholipid products activate Rac protein, a small G protein (Sohn *et al.*, 2000). Rac connects and activates PAK (p21-activated kinase). PAK-3 phosphorylates serine at position 338 on Raf-1 (Jaffer and Chernoff, 2002). The serine phosphorylation at this site is necessary for Raf-1 activation (Chiloeches *et al.*, 2001).

MEK is divided into MEK1 and MEK2 with a molecular weight of 44 kD and 45 kD (Crews *et al.*, 1992; Zheng and Guan, 1994). When Raf is activated, its C-terminal catalytic region can bind to MEK. Two Sers in the catalytic region were phosphorylated to activate MEK. MEK is a rare dual-specific kinase (Alberola-Ila and Hernández-Hoyos, 2003). ERK was activated by phosphorylation of tyrosine (Tyr) and Thr regulatory sites (Lai and Pelech, 2016). It is not clear how MEK possesses both Tyr and Thr bispecific phosphorylation activities (Butch and Guan, 1996). However, MEK has important physiological significance for Tyr/Thr bispecific phosphorylation of ERK (Wortzel and Seger, 2011). Because ERK signaling pathway plays a pivotal role in cell signal transduction network, any wrong activation will have a profound impact on cell life activities (Howe *et al.*, 2002). This dual-specific recognition and activation mechanism greatly improve the accuracy of signal transduction and prevent ERK from inaccurate activation (Roberts and Der, 2007).

4.1.2. PI3K/Akt/mTOR signaling pathway

Several reports showed that PI3K/Akt/mTOR signaling pathway plays an important role in cell proliferation, protein synthesis and angiogenesis (Chai *et al.*, 2018). The PI3K family can be divided into three categories, and the IA class in the family consists of two catalytic subunits, p110 and p85, as heterodimers of PI3K. Class IA can exert phosphatidylinositol kinase and protein kinase effects (Engelman *et al.*, 2006). Growth factors and cytokines outside the cell act as ligands that bind to transmembrane RTKs and activate RTKs. Furthermore, the substrate of RTKs is phosphorylated to recruit p85 subunits to the vicinity of the cell membrane (Mukohara, 2015). p85 regulates the subunit Src homology domain 2 (SH2), the heterodimer spatial conformation triggers the change, and the inhibition of the p110 subunit by the p85 subunit is abolished (Han *et al.*, 2018). The direct way of PI3K activation is regulated by the Ras superfamily (McCubrey *et al.*, 2007). The amino terminus of PI3K class I family members has the ability to bind to members of the Ras family. Ras protein can directly bind to p110 subunit after activation, enhancing enzyme activity (Sethi *et al.*, 1999). After PI3K activation, phosphatidylinositol-4,5-bisphosphate (PIP2) is phosphorylated to form phosphatidylinositol-3,4,5-triphosphate (PIP3) (Janku *et al.*, 2018). As a second messenger, PIP3 can be combined with Akt (Lee *et al.*, 2015). 3-phosphoinositide-dependent protein kinase-1 (PDK1) and 3-phosphoinositide-dependent protein kinase-2 (PDK2) phosphorylate the serine and threonine sites on Akt. Thus, Akt is fully activated (Chan and Tsichlis, 2001; Mercado-Pimentel *et al.*, 2016). In turn, the mammalian target of rapamycin (mTOR) signaling pathway is activated. As a result, PI3K/Akt/mTOR plays a key role in cell proliferation, differentiation, migration and many other aspects (Mitra *et al.*, 2012; Yu and Cui, 2016).

Phosphatase and tensin homolog (PTEN) is a PIP3-phosphatase, which is contrary to the function of PI3K (Gao *et al.*, 2000). It can convert PIP3 to PIP2 by dephosphorylation. PTEN can reduce the activation of Akt and blocks all downstream signal transduction events regulated by Akt (Zhao, 2007).

4.2. Transforming growth factor beta 1 (TGF-β1) signaling pathway

TGF-β1/Smad signal transduction pathway is a signal transduction pathway with multiple biological functions. Play an important role in tissue repair, tumor proliferation and metastasis, excessive fibrosis, etc (Al-Mulla *et al.*, 2011; Sun *et al.*, 2016). TGF-β1 is involved in the whole process of inflammation, proliferative phase, and plasticization during wound healing (Barrientos *et al.*, 2008; Crowe *et al.*, 2000). First, platelet degranulation releases TGF-β1 to the wound. TGF-β1 recruits monocytes and fibroblasts to reach the wound and maintains a high concentration of TGF-β1 by autocrine (Martin, 1997). The application of TGF-β1 can promote the recruitment and proliferation of fibroblasts in the wound site, accelerate the formation of new blood vessels, and enhance the ability of fibroblasts to synthesize extracellular matrix such as collagen (Lichtman *et al.*, 2016; Okizaki *et al.*, 2015; Puolakkainen *et al.*, 1995). And regulate the production of extracellular matrix (ECM) by adjusting the ratio of metalloproteinase (MMP)/MMP inhibitors (Chen *et al.*, 2003; Knittel *et al.*, 1999; Kuo *et al.*, 2005). In vitro experiments showed that TGF-β could activate fibroblasts to differentiate into myofibroblasts (Wynn and Vannella, 2016). In wound healing, it can promote wound contraction, ECM deposition and regulate the differentiation, proliferation, and maturation of epidermal keratinocytes (Ghosh *et al.*, 2017).

5. Purpose of this study

It has been reported that the aquatic extract of spirulina plays an important role in reducing oxidative damage and has wound healing potential for primary dermal fibroblasts (Li-Chen *et al.*, 2005; Syarina *et al.*, 2015). In addition, the proliferation of stem cells can also be promoted by spirulina (Bachstetter *et al.*, 2010). The crude extract of spirulina platensis combined with skin cream can promote the wound healing of human keratinocytes (HS2) and fibroblasts (L929) (Gunes *et al.*, 2017). Thus, the purpose of the present study was to determine the positive effect of SPCP on skin wound healing. The human dermal fibroblasts CCD-986sk cells were used to investigate the promoting effect of SPCP on cell proliferation and migration. The molecular mechanisms in this process were further revealed. In vivo study was performed, a mouse for full-thickness skin wounds on C57BL/6 mouse was used to further to determine the effect of SPCP on skin wound healing.

II. MATERIALS AND METHODS

1. Preparation of spirulina crude protein

Spirulina powder was purchased from New Zealand Nutritionals Ltd., (Burnside Christchurch, New Zealand) and soaked in distilled water at a concentration of 40 g/L. After churning up for 4 h at room temperature, the mixture was centrifugated at 2400 × g at 4 ℃ for 10 min. The supernatant was mixed with three volumes of ethanol. The mixture was centrifugated at 2400 × g at 4 ℃ for 10 min. The supernatant was subsequently filtered and concentrated using rotary evaporation at 40 ℃. The concentrated solution was precipitated with 80% saturated $(NH_4)_2SO_4$ at 4 ℃ overnight. The precipitate was dissolved in distilled water and dialyzed with dialysis membrane against distilled water. The dialysate was concentrated by using rotary evaporator at 40 ℃ and freeze-dried, then used as spirulina crude protein (SPCP) for subsequent experiments.

Sodium dodecyl sulfate-polyacrylamide gel electrophoresis (SDS-PAGE) and Coomassie brilliant blue methods were used to analyze SPCP protein profiles. SPCP (1300 μg/mL) was mixed with 5 × sample loading buffer (50 mM Tris-hydrochloride (Tris-HCl), 2% SDS, 10% glycerol, 0.02% bromophenol blue (BPB), 5% 2-mercaptoethanol), and then SPCP containing 75 μg protein were separated by 15% SDS-PAGE. Dyeing at room temperature with Coomassie Brilliant Blue for 1 h and washing with the destaining solution until the bands appear. The SPCP bands appearing at about 20 kDa and 16 kDa were analyzed using quadrupole time of flight mass spectrometry (Q-TOF MS/MS) provided by Peptron Corporation (Daejeon, Korea).

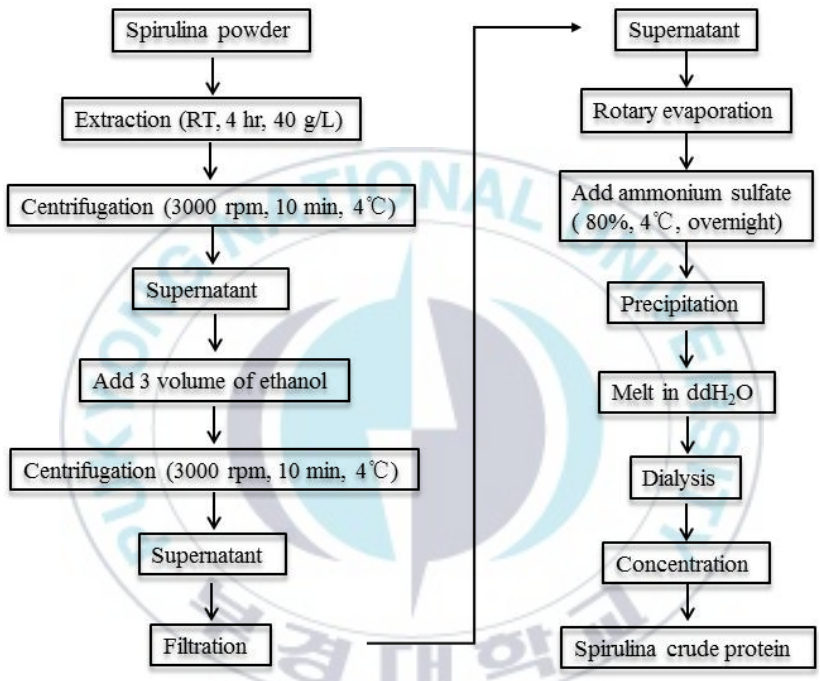

Figure 1. Preparation of SPCP.

2. In vitro assay

2.1. The effect of SPCP on the proliferation and migration of CCD-986sk cells

2.1.1. Cell culture

CCD-986sk human dermal fibroblast cell line (ATCC CRL-1947; American Type Culture Collection, Manassas, VA, USA) was obtained from normal female skin tissue. The cells were cultured in Dulbecco's Modified Eagle Medium (DMEM, Gibco; Thermo Fisher Science, Inc., Waltham, MA, USA), containing 10% fetal bovine serum (FBS, Gibco; Thermo Fisher Science, Inc.) and 1% penicillin and streptomycin in 37 ℃ and 5% carbon dioxide (CO_2) saturated wet incubator. CCD-986sk cells were cultured in a plate with a diameter of 100 mm to a confluence of 60-80%. The medium was replaced every 2 days.

2.1.2. Cell viability assay

Celltiter 96 AQueous One Solution Reagent (Promega Corporation, Madison, WI, USA) was used to determine cell viability. CCD-986sk cells were seeded into a 96-well plate with a density of 0.5×10^4 cells/well. After 24 h of incubation, serum-free medium (SFM) was used to incubate the cells for another 4 h at 37 ℃. The serum contains several hormones, which stimulates cell growth and masks the effect of SPCP, to avoid the complications, SFM was used in all groups (control group and SPCP treatment group). Subsequently, cells were treated with different concentrations of SPCP (6.25, 12.5 or 25 μg/mL in SFM) or SFM alone

(control). The cells were further cultured for 24 h. Subsequently, the cells were exposed to MTS analytical solution and cultured at 37 ºC for 30 min. The optical density at 490 nm was measured by Synergy HTX microplate reader (Biotek Instruments, Inc. Winooski, Vermont, USA). The data were expressed as the percentage of viable cells treated with SPCP compared with the viable cells treated with SFM.

2.1.3. BrdU assay

Cell Proliferation ELISA, BrdU (colorimetric) kit (Sigma-Aldrich; Merck KGaA, Darmstadt, Germany) was used to determine the proliferation of CCD-986sk cells. CCD-986sk cells were cultured under a standard condition. Cells were seeded into a 96-well plate at a confluence of 60%-80% with a density of 0.5×10^4 cells/well. After 24 h incubation, the culture medium was replaced with SFM and then incubated for another 4h at 37 ºC, then cells were treated with different concentrations of SPCP (0, 6.25, 12.5, and 25 μg/mL in SFM) for 24 h. Subsequently, each of the treated wells was added with 10 μL of BrdU labeling solution and then incubated at 37 ºC for 2 h, then the BrdU labeling medium was replaced with 200 μL of FixDenat. The cells were incubated at room temperature for 30 min, and the FixDenat was replaced by 100 μL of anti-BrdU-POD working solution. The cells were incubated at room temperature for 90 min, and then each well was washed with 200 μL of washing solution (phosphate-buffered saline (PBS)) three times. Ultimately, 100 μL of Substrate solution was added, and the plate was incubated at room temperature for 5-30min until the color is sufficient for photometric detection. Synergy HTX microplate reader (BioTek Instruments, Inc., Winooski, VT, USA) was used to measure the absorbance at 370 and 492 nm. The data were expressed as a

percentage of absorbance ($A_{370\ nm}$-$A_{492\ nm}$) in different concentrations of SPCP-treated cells compared with the SFM-treated control.

2.1.4. The measurement of elastase activity

N-succinyl-Ala-Ala-p-nitroaniline (Sigma-Aldrich; Merck Kgaa, Darmstadt, Germany) was used to measure the elastase activity of CCD-986sk cells. The CCD-986sk cells were seeded into 6-well plates at a density of 5×10^4 cells/well. After 24 h of incubation, the cells were cultured with SFM incubated at 37 ºC for another 4 h. Cells were treated with different concentrations of SPCP (6.25, 12.5 or 25 μg/mL in SFM) or SFM alone (control group), and further cultured for another 24 h. Cells were collected in radio-immunoprecipitation analysis buffer (iNtRON Biotechnology, Seongnam, Korea) which contains 1% protease inhibitor using cell scraper. Cell lysates were collected by centrifugation at 16000 × g for 10 min at 4 ºC. Then the supernatant (98 μL) and 25 mg/mL N-succinyl-Ala-Ala-Ala-p-nitroaniline (2 μL) were added to each well. After incubation at 37 ºC for 30 min, the collaborative HTX microplate reader (BioTek Instr uments, Inc.) was used to measure the optical density at 410 nm. The data were expressed as the percentage of elastase activity in the SPCP-treated cells compared with the elastase activity in the cells treated with SFM alone.

2.1.5. Procollagen type I C-peptide (PIP) solid phase enzyme immunoassay

The level of collagen was determined by Takara MK101 kit (Takara Bio, Inc., Otsu, Japan). Cell density was 5×10^4 cells/well, seeded in 6-well plate. After 24 h of incubation, these cells were incubated with SFM for 4 h at 37 ºC. And then

followed by an additional 24 h with different concentrations of SPCP (6.25, 12.5, or 25 μg/mL) or SFM (control). Cell medium was collected and then centrifuged at 16000 × g at 4 ºC for 10 min. Subsequently, 100 μL antibody-peroxidase conjugation solutions and 20 μL supernatant were added to each well. After incubation for 3 h at 37 ºC, each test well was washed by 400 μL of PBS for four times. 100 μL of 3, 3, 5, 5'- tetramethylbenzidine substrate solution was added to each well and incubated at room temperature for 15 min. The reaction was terminated by adding 100 μL of stop solution (1 N sulfuric acid (H_2SO_4)). Absorption at 450 nm was measured using Synergy HTX microplate reader (BioTek Instruments, Inc.).

2.1.6. Wound healing assay

CCD-986sk cells were cultured under standard culture conditions and seeded in six-well plates at a confluence of 60-80%. The medium was changed every 2 days. After confluence, the culture medium was replaced with SFM and incubated for another 4 h. A layered wound was scraped by using sterile 200 μL plastic pipette tip in the center of the well. The cells were washed twice by using PBS and cell debris was removed. SPCP (0, 6.25, 12.5, 25 μg/mL) of different concentrations were used to treat the wounds for 24 h. The wounds were photographed with a digital camera inverted microscope at 0 and 24 h, respectively. Image J software was used (version 1.40; National Institutes of Health, Bethesda, MD, USA) to measure the size of the wound. It was expressed as the percentage of the final distance and the initial distance of the wound.

2.1.7. Cell cycle analysis

BD Cycletest TM Plus DNA Reagent Kit (Becton, Dikinson, and company) was used to determine the cell cycle progress by flow cytometry. Cells were cultured in DMEM medium and replaced with SFM at a confluence of 40%-60%. After 4 h incubation at 37 ºC, cells were treated with different concentrations of SPCP (0, 6.25, 12.5, 25 μg/mL) for another 24 h at 37 ºC. Buffer Solution was used to harvest, and wash the cells for two times. The concentration of the cells was counted and adjusted to 1.0×10^6 cells/mL with Buffer Solution. Cells were centrifuged. And then the supernatant was discarded. Solution A (trypsin buffer) was added and mixed with the cells. After incubation for 10 min at room temperature (20-25 ºC), solution B (trypsin inhibitor and RNase buffer) was added, and the mixture was incubated for another 10 min at room temperature (20-25 ºC). Ultimately, solution C (propidium iodide (PI) stain solution) was added. And the cells were incubated for 10 min in the dark on ice. The BD FACSVerseTM system (Becton, Dickinson and Company, USA) was used to detect the cell cycle. And the software of ModFit (version 3.1; Verity Software House, Topsham, ME, USA) was used to analyze the cell cycle data.

2.1.8. Preparation of whole cell lysates

CCD-986sk cells were cultured under standard conditions and treated as described above. After treatment, cells were washed with PBS two times. And radioimmunoprecipitation lysis buffer (RIPA buffer, iNtRON Biotechnology) with 1% protease inhibitor was used to lysis the cells at 4 ºC for 30 min. Cells were harvested by scraping on ice. The cell lysate was centrifuged at 16000 × g for 10 min at 4 ºC. The supernatant was collected as the protein. Bicinchoninic acid (BCA) protein assay kit (Pierce; Thermo Fisher Scientific, Inc.) was used to analyze the concentration of the protein. The protein concentration of different treatment groups

was adjusted to the same level. After that, the protein solution was mixed with sodium dodecyl sulfate (SDS) sample buffer containing dithiothreitol (DTT) and denatured at 100 ºC for 5 min.

2.1.9. Western blot analysis

The SDS-PAGE gel was used to separate proteins, and the proteins were transferred to polyvinylidene difluoride (PVDF) membranes (Millipore, Milford, CT, USA). Membranes were washed with methanol and then blocked for 2 h with Tris-buffered saline with 0.1% tween 20 (TBS-T, 10mm Tris-HCl, 150mm NaCl (pH 7.5) and 0.1% Tween-20) containing 1% bovine serum albumin (BSA). The membrane was incubated at 4 ºC overnight in the primary antibody. After washing two times with TBS-T for 15 min each time, the membrane was incubated at room temperature for another 2 h. The second antibodies were horseradish peroxidase (HRP)-conjugated anti-rabbit Immunoglobulin G (IgG) (Cell Signaling Technology, Inc., Beverly, MA, USA, cat. no. 7074S), donkey anti-goat IgG (Bethyl Laboratories, Inc., Beverly, MA, USA, cat. no. A50-101p), and anti-mouse IgG (Cell Signaling Technology, Inc., cat. no. 7076S). The primary antibodies were showed in Table 1. The color development was determined using an enhanced chemiluminescence western blot kit (Thermo Fisher Scientific, Rockford, IL, USA). The bioanalytical imaging system (Azure Biosystems, Dublin, CA, USA) was used to detect the protein bands. The Multi-Gauge software, version 3.0 (Fujifilm Life Science, Tokyo, Japan) was used to analyze the density of the protein bands. Each density of the protein bands was normalized to GAPDH.

2.2. SPCP activates the EGFR/ERK signaling pathway in the proliferation and migration of CCD-986sk cells

2.2.1. Cell culture

CCD-986sk human dermal fibroblast cell line (ATCC CRL-1947; American Type Culture Collection, Manassas, VA, USA) was obtained from normal female skin tissue. The cells were cultured in DMEM medium (Gibco; Thermo Fisher Science, Inc., Waltham, MA, USA), containing 10% FBS (Gibco; Thermo Fisher Science, Inc.) and 1% penicillin and streptomycin in 37 ºC and 5% CO_2 saturated wet incubator. CCD-986sk cells were cultured in a plate with a diameter of 100 mm to a confluence of 60-80%. The medium was replaced every 2 days.

2.2.2. Cell viability assay

Celltiter 96 AQueous One Solution Reagent (Promega Corporation, Madison, WI, USA) was used to determine cell viability. CCD-986sk cells were seeded into a 96-well plate with a density of 0.5×10^4 cells/well. After 24 h of incubation, SFM was used to incubate the cells for another 4 h at 37 ºC. The serum contains several hormones, which stimulates cell growth and masks the effect of SPCP, to avoid the complications, SFM was used in all groups (control group and SPCP treatment group). Subsequently, cells were treated with different concentrations of SPCP (6.25, 12.5 or 25 μg/mL in SFM) or SFM alone (control). The cells were further cultured for 24 h. Subsequently, the cells were exposed to MTS analytical solution and cultured at 37 ºC for 30 min. The optical density at 490 nm was measured by Synergy HTX microplate reader (Biotek Instruments, Inc.

Winooski, Vermont, USA). The data were expressed as the percentage of viable cells treated with SPCP compared with the viable cells treated with SFM.

2.2.3. BrdU assay

Cell Proliferation ELISA, BrdU (colorimetric) kit (Sigma-Aldrich; Merck KGaA, Darmstadt, Germany) was used to determine the proliferation of CCD- 986sk cells. CCD-986sk cells were cultured under a standard condition. Cells were seeded into a 96-well plate at a confluence of 60%-80% with a density of 0.5×10^4 cells/well. After 24 h incubation, the culture medium was replaced with SFM and incubated for another 4h at 37 ºC, then cells were treated with different concentrations of SPCP (0, 6.25, 12.5, and 25 μg/mL in SFM) for 24 h. Subsequently, each of the treated wells was added with 10 μL of BrdU labeling solution and then incubated at 37 ºC for 2 h. Then the BrdU labeling medium was replaced with 200 μL of FixDenat. The cells were incubated at room temperature for 30 min, and the FixDenat was replaced by 100 μL of anti-BrdU-POD working solution. The cells were incubated at room temperature for 90 min, and then each well was washed with 200 μL of washing solution (PBS) for three times. Ultimately, 100 μL of Substrate solution was added, and the plate was incubated at room temperature for 5-30min until the color was sufficient for photometric detection. Synergy HTX microplate reader (BioTek Instruments, Inc., Winooski, VT, USA) was used to measure the absorbance at 370 and 492 nm. The data were expressed as a percentage of absorbance ($A_{370\ nm}$-$A_{492\ nm}$) in different concentrations of SPCP-treated cells compared with the SFM-treated cells.

2.2.4. Wound healing assay

CCD-986sk cells were cultured under standard culture conditions and seeded in six-well plates at a confluence of 60-80%. The medium was changed every 2 days. After confluence, the culture medium was replaced with SFM and incubated for another 4 h. A layered wound was scraped by using sterile 200 μL plastic pipette tip in the center of the well. The cells were washed twice by using PBS and cell debris was removed. Different concentrations of SPCP (0, 6.25, 12.5, 25 μg/mL) were used to treat the wounds for 24 h. The wounds were photographed with a digital camera inverted microscope at 0 and 24 h, respectively. Image J software was used (version 1.40; National Institutes of Health, Bethesda, MD, USA) to measure the size of the wound. It was expressed as the percentage of the final distance and the initial distance of the wound.

2.2.5. The treatment of inhibitor

For inhibitor treatment, the MEK inhibitor U0126 was used in the present study. After incubation with SFM for 4 h, the cells were treated with 10 μmol/L of U0126 for 1 h. And then the cells were treated with different concentrations of SPCP (0, 6.25, 12.5, 25 μg/mL) for 24 h as described above.

2.2.6. Preparation of whole cell lysates

CCD-986sk cells were cultured under standard conditions and treated as described above. After treatment, cells were washed with PBS two times. And RIPA buffer (iNtRON Biotechnology) with 1% protease inhibitor was used to lysis cells at 4 ºC for 30 min. Cells were harvested by scraping on ice. The cell lysate was centrifuged at 16000 × g for 10 min at 4 ºC. The supernatant was collected as the protein. BCA protein assay kit (Pierce; Thermo Fisher Scientific, Inc.) was used to

analyze the concentration of the protein. The protein concentration of different treatment groups was adjusted to the same level. After that, the protein solution was mixed with SDS sample buffer containing DTT and denatured at 100 ºC for 5 min.

2.2.7. Western blot analysis

The SDS-PAGE gel was used to separate proteins, and the proteins were transferred to PVDF membranes (Millipore, Milford, CT, USA). Membranes were washed with methanol and then blocked for 2 h with TBS-T (10mm Tris-HCl, 150mm NaCl (pH 7.5) and 0.1% Tween-20) containing 1% BSA. The membrane was incubated at 4 ºC overnight in the primary antibody. After washing two times with TBS-T for 15 min each time, the membrane was incubated at room temperature for another 2 h. The second antibodies were HRP-conjugated anti-rabbit IgG (Cell Signaling Technology, Inc., Beverly, MA, USA, cat. no. 7074S), donkey anti-goat IgG (Bethyl Laboratories, Inc., Beverly, MA, USA, cat. no. A50-101p), and anti-mouse IgG (Cell Signaling Technology, Inc., cat. no. 7076S). The primary antibodies were showed in Table 1. The color development was determined using an enhanced chemiluminescence western blot kit (Thermo Fisher Scientific, Rockford, IL, USA). The bioanalytical imaging system (Azure Biosystems, Dublin, CA, USA) was used to detect the protein bands. The Multi-Gauge software, version 3.0 (Fujifilm Life Science, Tokyo, Japan) was used to analyze the density of the protein bands. Each density of the protein bands was normalized to GAPDH.

2.3. SPCP activates the PI3K/Akt signaling pathway in the proliferation and migration of CCD-986sk cells

2.3.1. Cell culture

CCD-986sk human dermal fibroblast cell line (ATCC CRL-1947; American Type Culture Collection, Manassas, VA, USA) was obtained from normal female skin tissue. The cells were cultured in DMEM medium (Gibco; Thermo Fisher Science, Inc., Waltham, MA, USA), containing 10% FBS (Gibco; Thermo Fisher Science, Inc.) and 1% penicillin and streptomycin in 37 ºC and 5% CO_2 saturated wet incubator. CCD-986sk cells were cultured in a plate with a diameter of 100 mm to a confluence of 60-80%. The medium was replaced every 2 days.

2.3.2. Cell viability assay

Celltiter 96 AQueous One Solution Reagent (Promega Corporation, Madison, WI, USA) was used to determine cell viability. CCD-986sk cells were seeded into a 96-well plate with a density of 0.5×10^4 cells/well. After 24 h of incubation, SFM was used to incubate the cells for another 4 h at 37 ºC. The serum contains several hormones, which stimulates cell growth and masks the effect of SPCP, to avoid the complications, SFM was used in all groups (control group and SPCP treatment group). Subsequently, cells were treated with different concentrations of SPCP (6.25, 12.5 or 25 μg/mL in SFM) or SFM alone (control). The cells were further cultured for 24 h. Subsequently, the cells were exposed to MTS analytical solution and cultured at 37 ºC for 30 min. The optical density at 490 nm was measured by Synergy HTX microplate reader (Biotek Instruments, Inc. Winooski, Vermont, USA). The data were expressed as the percentage of viable cells treated with SPCP compared with the viable cells treated with SFM.

2.3.3. BrdU assay

Cell Proliferation ELISA, BrdU (colorimetric) kit (Sigma-Aldrich; Merck KGaA, Darmstadt, Germany) was used to determine the proliferation of CCD-986sk cells. CCD-986sk cells were cultured under a standard condition. Cells were seeded into a 96-well plate at a confluence of 60%-80% with a density of 0.5×10^4 cells/well. After 24 h incubation, the culture medium was replaced with SFM and then incubated for another 4h at 37 ºC, then cells were treated with different concentrations of SPCP (0, 6.25, 12.5, and 25 μg/mL in SFM) for 24 h. Subsequently, each of the treated wells was added with 10 μL of BrdU labeling solution and then incubated at 37 ºC for 2 h, then the BrdU labeling medium was replaced with 200 μL of FixDenat. The cells were incubated at room temperature for 30 min, and the FixDenat was replaced by 100 μL of anti-BrdU-POD working solution. The cells were incubated at room temperature for 90 min, and then each well was washed with 200 μL of washing solution (PBS) for three times. Ultimately, 100 μL of Substrate solution was added. And the plate was incubated at room temperature for 5-30min until the color was sufficient for photometric detection. Synergy HTX microplate reader (BioTek Instruments, Inc., Winooski, VT, USA) was used to measure the absorbance at 370 and 492 nm. The data were expressed as a percentage of absorbance ($A_{370\ nm}$-$A_{492\ nm}$) in different concentrations of SPCP-treated cells compared with the SFM-treated cells.

2.3.4. Wound healing assay

CCD-986sk cells were cultured under standard culture conditions and seeded in six-well plates at a confluence of 60-80%. The medium was changed every 2 days. After confluence, the culture medium was replaced with SFM and incubated for another 4 h. A layered wound was scraped by using sterile 200 μL plastic pipette

tip in the center of the well. The cells were washed twice by using PBS and cell debris was removed. Different concentrations of SPCP (0, 6.25, 12.5, 25 μg/mL) were used to treat the wounds for 24 h. The wounds were photographed with a digital camera inverted microscope at 0 and 24 h, respectively. Image J software was used (version 1.40; National Institutes of Health, Bethesda, MD, USA) to measure the size of the wound. It was expressed as the percentage of the final distance and the initial distance of the wound.

2.3.5. The treatment of inhibitor

For inhibitor treatment, the Akt inhibitor LY294002 was used in the present study. After incubation with SFM for 4 h, the cells were treated with 50 μmol/L of LY294002 for 1 h. And then the cells were treated with different concentrations of SPCP (0, 6.25, 12.5, 25 μg/mL) for 24 h as described above.

2.3.6. Preparation of whole cell lysates

CCD-986sk cells were cultured under standard conditions and treated as described above. After treatment, cells were washed with PBS two times. And RIPA buffer (iNtRON Biotechnology) with 1% protease inhibitor was used to lysis cells at 4 ºC for 30 min. Cells were harvested by scraping on ice. The cell lysate was centrifuged at 16000 × g for 10 min at 4 ºC. The supernatant was collected as the protein. BCA protein assay kit (Pierce; Thermo Fisher Scientific, Inc.) was used to analyze the concentration of the protein. The protein concentration of different treatment groups was adjusted to the same level. After that, the protein solution was mixed with SDS sample buffer containing DTT and denatured at 100 ºC for 5 min.

2.3.7. Preparation of nuclear and cytoplasmic lysates

CCD-986sk cells were treated according to the above methods. According to the manufacturer's instructions, the NE-PER Nuclear and Cytoplasmic Extraction Reagents (Pierce Biotechnology, Inc., Rockford, IL, USA) was used to separate nuclear and cytoplasmic extracts. BCA protein assay kit (Pierce; Thermo Fisher Scientific, Inc.) was used to analyze the concentration of the protein. The protein concentration of different treatment groups was adjusted to the same level. After that, the protein solution was mixed with SDS sample buffer containing DTT and denatured at 100 ºC for 5 min.

2.3.8. Western blot analysis

The SDS-PAGE gel was used to separate proteins, and the proteins were transferred to PVDF membranes (Millipore, Milford, CT, USA). Membranes were washed with methanol and then blocked for 2 h with TBS-T (10mm Tris-HCl, 150mm NaCl (pH 7.5) and 0.1% Tween-20) containing 1% BSA. The membrane was incubated at 4 ºC overnight in the primary antibody. After washing two times with TBS-T for 15 min each time, the membrane was incubated at room temperature for another 2 h. The second antibodies were HRP-conjugated anti-rabbit IgG (Cell Signaling Technology, Inc., Beverly, MA, USA, cat. no. 7074S), donkey anti-goat IgG (Bethyl Laboratories, Inc., Beverly, MA, USA, cat. no. A50-101p), and anti-mouse IgG (Cell Signaling Technology, Inc., cat. no. 7076S). The primary antibodies were showed in Table 1. The color development was determined using an enhanced chemiluminescence western blot kit (Thermo Fisher Scientific, Rockford, IL, USA). The bioanalytical imaging system (Azure Biosystems, Dublin, CA, USA) was used to detect the protein bands. The Multi-Gauge software, version 3.0 (Fujifilm Life

Science, Tokyo, Japan) was used to analyze the density of the protein bands. Each density of the protein bands was normalized to GAPDH.

3. In vivo assay

3.1. Experimental animals

Six weeks old male C57BL/6 mice were obtained from IDEXX bioresearch (South Korean) and maintained in controlled conditions with proper temperature (22ºC) and humidity (40%-45%) under a light/dark cycle of 12 h/12 h. They were kept in single-house and fed with standard rodent food and water *ad libitum*.

3.2. Full thickness excisional wounds

All experiments procedures were approved by the University Animal Care and Use Committee guidelines at Pukyong National University (Busan, Korea) (Approval NO. 2018-15) and conducted according to the international regulations of the usage and welfare of laboratory animals. The mice were allowed to adapt to the new environment for 1 week. Mice were anesthetized with ether. The hair of the dorsal surface was removed by an electric clipper. Each mouse dorsal skin was rinsed using alcohol, and then 8-mm-diameter biopsy punch was used to create a full-thickness wound on the back of the mouse. All of the mice were randomly divided into four groups for 5 mice in each group. The first group was the control group with the treatment of Vaseline only. The second group was a positive control group with the treatment of Vaseline containing 10 μg/g EGF. The third group was a sample group with the treatment of Vaseline containing 2% SPCP. The fourth group was a

sample group with the treatment of Vaseline containing 4% SPCP. Vaseline, EGF or SPCP was applied directly to the wound site once per day. The healing of the wound was macroscopically monitored by taking pictures with a digital camera at one o'clock p.m. every day. The mice were anesthetized with ether and sacrificed after nine days of treatment. The skin around the wound was collected and treated with liquid nitrogen. The collected skin tissues were stored at -70 ºC for subsequent experiments. The wound areas were calculated using Image J software (version 1.40; National Institutes of Health, Bethesda, MD, USA). It was expressed as the percentage of the original size.

3.3. Measurement of SOD activity

The SOD Activity Assay Kit (BioVision, Milpitas Boulevard, Milpitas, CA 95035 USA) was used to determine the activity of SOD in mice skin tissue. Firstly, PBS was used to remove any red blood cells. The skin tissue was homogenized with ice-cold 0.1 mol/L of Tris/HCl (pH 7.4, containing 5 mmol/L of β-Mercaptoethanol (β-ME), 0.5% Triton X-100 and 0.1 mg/mL phenylmethylsulfonyl fluoride (PMSF)). After that, it was centrifuged at 14,000 × g for 5 min at 4 ºC. The supernatant was used to determine the activity of SOD. Setting up 4 groups in 96-well plate. Such as sample, blank 1, blank 2 and blank 3. 20 μL of sample solution was added to each well of sample group and blank 2 group, respectively. Add 20 μL of ddH_2O to each well of blank 1 group and blank 3 group, respectively. Each of the above wells was added with 200 μL of Dilution Buffer. Add 20 μL of Enzyme Working Solution to each well of the sample group and blank 1 group. The plate was incubated at 37 ºC for 20 min. Synergy HTX microplate reader (BioTek Instruments, Inc., Winooski,

VT, USA) was used to measure the absorbance at 450 nm. The activity of SOD was calculated according to the manufacturer's instructions.

3.4. Measurement of CAT activity

The activity of CAT was determined using Catalase Activity Colorimetric/Fluorometric Assay Kit (BioVision, Milpitas Boulevard, Milpitas, CA 95035 USA). The skin tissue was homogenized with ice-cold Assay Buffer. After that, it was centrifuged at 10,000 × g for 5 min at 4 ºC. The supernatant was used to determine the activity of CAT. Each of the sample wells was added with 50 μL of Sample Solution and the positive control well was added with 3 μL of Positive Control Solution. Each of the wells was added with Assay Buffer to the final volume of 78 μL. The Sample High Control well was added with 50 μL of the sample solution and then added with Assay Buffer to the final volume of 78 μL. The Sample High Control well was then added with 10 μL of Stop Solution. After mixed, the plate was incubated at 25 ºC for 5 min to inhibit the activity of CAT adequately. Followed by adding 12 μL of 1 mmol/L H_2O_2 to each well (sample well, positive control well and sample high control well). The plate was incubated at 25 ºC for 30 min. After that, 10 μL of Stop Solution was added to the sample well and positive control well. 50 μL of Develop Mix (46 μL of Assay Buffer, 2 μL of OxiRed™ Probe and 2 μL of HRP solution) was added to each well and incubated at 25 ºC for 10 min. Synergy HTX microplate reader (BioTek Instruments, Inc., Winooski, VT, USA) was used to measure the absorbance at 570 nm. The activity of CAT was calculated according to the manufacturer's instructions.

3.5. Measurement of MDA level

The level of MDA was determined using Lipid Peroxidation (MDA) Colorimetric/Fluorometric Assay Kit (BioVision, Milpitas Boulevard, Milpitas, CA 95035 USA). The skin tissue was homogenized with MDA Lysis Buffer. After that, it was centrifuged at 13,000 × g for 10 min. 200 μL of supernatant was taken in a 1.5 mL microcentrifuge tube. 600 μL of thiobarbituric acid (TBA) was added to each well and incubated at 95 ºC for 60 min. The sample was placed in the ice for 10 min and thawed to the room temperature. 200 μL was taken from 800 μL reaction mixture to 96-well plate for analysis. Synergy HTX microplate reader (BioTek Instruments, Inc., Winooski, VT, USA) was used to measure the absorbance at 532 nm. The level of MDA was calculated according to the manufacturer's instructions.

3.6. Preparation of whole cell lysates

Skin tissue was minced and homogenized using RIPA buffer (iNtRON Biotechnology) with 1% protease inhibitor in an ice-bath. After that, the extract was incubated in ice and then centrifuged at 16000 × g for 10 min at 4 ºC. The supernatant was collected as the protein. BCA protein assay kit (Pierce; Thermo Fisher Scientific, Inc.) was used to analyze the concentration of the protein. The protein concentration of different treatment groups was adjusted to the same level. After that, the protein solution was mixed with SDS sample buffer containing DTT and denatured at 100 ºC for 5 min.

3.7. Western blot analysis

The SDS-PAGE gel was used to separate proteins. And the proteins were transferred to PVDF membranes (Millipore, Milford, CT, USA). Membranes were washed with methanol and then blocked for 2 h with TBS-T (10mm Tris-HCl,

150mm NaCl (pH 7.5) and 0.1% Tween-20) containing 1% BSA. The membrane was incubated at 4 ºC overnight in the primary antibody. After washing two times with TBS-T for 15 min each time, the membrane was incubated at room temperature for another 2 h. The second antibodies were HRP-conjugated anti-rabbit IgG (Cell Signaling Technology, Inc., Beverly, MA, USA, cat. no. 7074S), donkey anti-goat IgG (Bethyl Laboratories, Inc., Beverly, MA, USA, cat. no. A50-101p), and anti-mouse IgG (Cell Signaling Technology, Inc., cat. no. 7076S). The primary antibodies were showed in Table 1. The color development was determined using an enhanced chemiluminescence western blot kit (Thermo Fisher Scientific, Rockford, IL, USA). The bioanalytical imaging system (Azure Biosystems, Dublin, CA, USA) was used to detect the protein bands. The software of Multi-Gauge software, version 3.0 (Fujifilm Life Science, Tokyo, Japan) was used to analyze the density of these protein bands. Each density of these protein bands was normalized to GAPDH.

4. Statistical analysis.

For all assays, at least three independent experiments were performed. The mean ± standard deviations of the expression values were calculated using Microsoft Excel. The differences between two groups were evaluated with one-way analysis of variance followed by Bonferroni post hoc test using SPSS statistical software for Windows, v.20.0 (IBM Corp., Armonk, NY, USA).

Table 1. Primary antibodies used in western blot analysis

Name of Primary Antibody	Manufacturer and Catalog NO.	Dilution Rate
GAPDH	Santa Cruz Biotechnology: sc-25778	1:1000
MMP8	Santa Cruz Biotechnology: sc-8848	1:1000
Cdk 2	Santa Cruz Biotechnology: sc-163	1:1000
Cdk 4	Santa Cruz Biotechnology: sc-601	1:1000
Cdk 6	Santa Cruz Biotechnology: sc-177	1:1000
cyclin D1	Santa Cruz Biotechnology: sc-8396	1:1000
cyclin E	Santa Cruz Biotechnology: sc-481	1:1000
pRb	Santa Cruz Biotechnology: sc-377528	1:1000
p21	Santa Cruz Biotechnology: sc-271532	1:1000
p27	Santa Cruz Biotechnology: sc-528	1:1000
p-EGFR	Santa Cruz Biotechnology: sc-12351	1:1000
EGFR	Santa Cruz Biotechnology: sc-03	1:1000
SHC	Santa Cruz Biotechnology: sc-967	1:1000
GRB2	Santa Cruz Biotechnology: sc-255	1:1000
SOS	Santa Cruz Biotechnology: sc-259	1:1000
Ras	Santa Cruz Biotechnology: sc-520	1:1000
p-MEK	Santa Cruz Biotechnology: sc-81503	1:500
MEK	Santa Cruz Biotechnology: sc-81504	1:1000
p-ERK	Santa Cruz Biotechnology: sc-7383	1:1000
ERK1	Santa Cruz Biotechnology: sc-271269	1:1000

Name of Primary Antibody	Manufacturer and Catalog NO.	Dilution Rate
ERK2	Santa Cruz Biotechnology: sc-154	1:1000
p-p8α	Santa Cruz Biotechnology: sc-12929	1:500
p8α	Santa Cruz Biotechnology: sc-1637	1:500
P110	Santa Cruz Biotechnology: sc-8010	1:500
p-Akt	Santa Cruz Biotechnology: sc-514032	1:500
Akt	Santa Cruz Biotechnology: sc-8312	1:500
PTEN	Santa Cruz Biotechnology: sc-7974	1:1000
p-mTOR	Santa Cruz Biotechnology: sc-293132	1:500
mTOR	Santa Cruz Biotechnology: sc-8319	1:500
p-p70S6K	Santa Cruz Biotechnology: sc-8416	1:1000
p70S6K	Santa Cruz Biotechnology: sc-8418	1:1000
p-4EBP1	Santa Cruz Biotechnology: sc-293124	1:1000
4EBP1	Santa Cruz Biotechnology: sc-9977	1:500
eIF4E	Santa Cruz Biotechnology: sc-514875	1:500
β-Actin	Santa Cruz Biotechnology: sc-47778	1:1000
Lamin B1	Santa Cruz Biotechnology: sc-377000	1:1000
p-GSK3β	Santa Cruz Biotechnology: sc-373800	1:1000
GSK3β	Santa Cruz Biotechnology: sc-377213	1:1000
β-catenin	Santa Cruz Biotechnology: sc-1496	1:1000
α-Actin	Santa Cruz Biotechnology: sc-32251	1:1000
TGFβ1	Santa Cruz Biotechnology: sc-146	1:1000
p-Smad2	Santa Cruz Biotechnology: sc-135644	1:1000
Smad2	Santa Cruz Biotechnology: sc-6200	1:1000

COL1A1	Santa Cruz Biotechnology: sc-293182	1:500
COL1A2	Santa Cruz Biotechnology: sc-376350	1:500

III. RESULTS AND DISCUSSION

1. Preparation of spirulina crude protein

The crude extract from spirulina is a complex mixture of proteins. The proteins were separated by SDS-PAGE and then stained with Coomassie Brilliant Blue. There were two bands revealing at about 20 and 16 kDa, respectively (Fig. 2). From the analysis of Q-TOF MS/MS, the band at about 16 kDa was C-phycocyanin α chain while the band at about 20 kDa didn't correspond to any known protein.

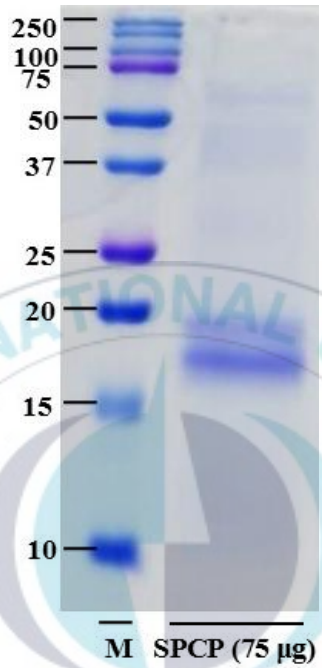

Figure 2. Protein profile of SPCP. SPCP was loaded on a 15% polyacrylamide gel and stained with Coomassie Brilliant Blue. M, marker

2. Effect of SPCP on the proliferation and migration of CCD-986sk cells

2.1. Effect of SPCP on the cell viability of CCD-986sk cells

To investigate the effects of SPCP on the viability of CCD-986sk cells, an MTS assay on cells treated with various doses of SPCP was performed. The results showed that SPCP improved cell viability in a dose-dependent manner. There was an 18%, 33% and 42% increase in cell viability over the control at 6.25, 12.5 and 25 μg/mL of SPCP, respectively (Fig. 3). These results demonstrated that SPCP can effectively enhance the cell viability of human fibroblast CCD-986sk cells at specific doses.

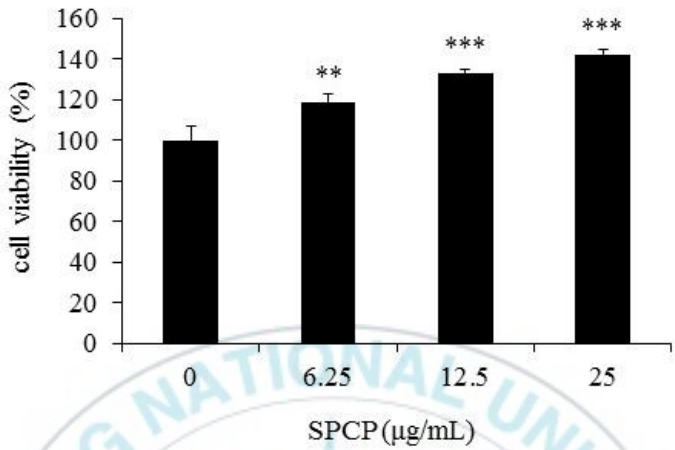

Figure 3. The treatment of SPCP stimulated the viability of CCD-986sk cells. Cell viability was determined by MTS assay following treatment with various concentrations of SPCP for 24 h. SPCP effectively enhanced the cell viability of human fibroblast CCD-986sk cells. Each value represents the mean ± standard deviation of three independent experiments. ** $p < 0.01$, *** $p < 0.001$ compared to the control group.

2.2. Effect of SPCP on the cell proliferation of CCD-986sk cells

In order to further determine the effect of SPCP on the proliferation of CCD-986sk cells, BrdU assay was performed. As shown in Figure 4, The results showed that after being treated with 6.25 μg/mL, 12.5 μg/mL, or 25 μg/mL SPCP, the ratio of BrdU incorporation in CCD-986sk cells was significantly increased by 0.9 ± 0.31 ($P < 0.05$), 1.5 ± 0.4 ($P < 0.01$), and 3.1 ± 0.38 ($P < 0.001$). Therefore, this result indicated that SPCP promoted the proliferation of CCD-986sk cells in a dose-dependent manner.

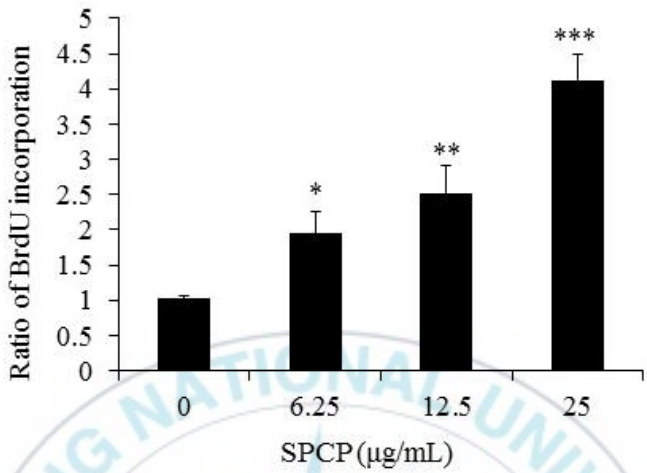

Figure 4. The treatment of SPCP enhanced the proliferation of CCD-986sk cells. CCD-986sk cells were incubated with various concentrations of SPCP for 24 h and then the cell proliferation was determined by BrdU assay. SPCP promoted the proliferation of CCD-986sk cells in a dose-dependent manner. Each value represents the mean ± standard deviation of three independent experiments. * $p < 0.05$, ** $p < 0.01$, *** $p < 0.001$ compared to the control group.

2.3. Effect of SPCP on the activity of elastase

In order to explore the effect of SPCP treatment on the elastase activity of CCD-986sk cells, the activity of elastase was determined by ELISA. Compared with the control, SPCP treatment significantly decreased the elastase activity in a dose-dependent manner ($P < 0.05$ or $P < 0.001$; Fig. 5), with a maximum decrease of 42 ± 6.15% observed in cells treated with 25 μg/ml SPCP.

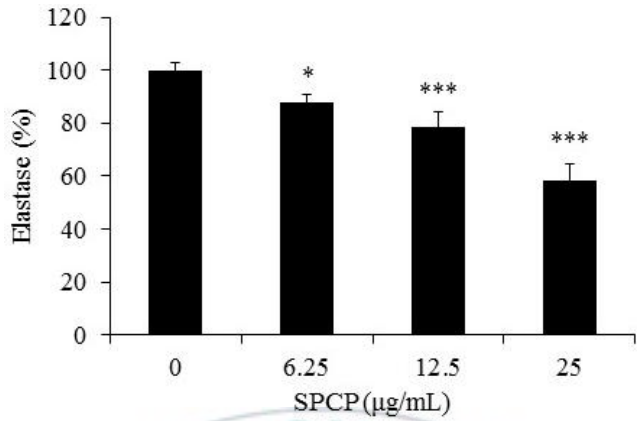

Figure 5. The treatment of SPCP reduced the activity of elastase in CCD-986sk cells. The activity of elastase was determined by the ELISA assay following treatment with various concentrations of SPCP for 24 h. SPCP significantly decreased the elastase activity in a dose-dependent manner. Each value represents the mean ± standard deviation of three independent experiments. * $p < 0.05$, *** $p < 0.001$ compared to the control group.

2.4. Effect of SPCP on PIP levels

To determine whether SPCP affects the secretion of type I procollagen, secreted levels of PIP were measured by ELISA. The results showed that SPCP markedly increased the level of PIP in a dose-dependent manner in CCD-986sk cells. Compared with the basal level of 77 ng/mL, there were 100, 121 and 187 ng/mL of PIP induced by 6.25, 12.5 and 25 μg/mL of SPCP, respectively (Fig. 6).

In order to determine the effect of SPCP on the expression level of MMP-8 in CCD-986sk cells, western blot analysis was performed. As shown in Figure 7, the expression level of MMP-8 protein weas significantly decreased by SPCP in a dose-dependent manner. These results demonstrated that SPCP can effectively protect collagen against destruction by controlling the synthesis of collagen and inhibiting the degradation of collagen by MMP-8.

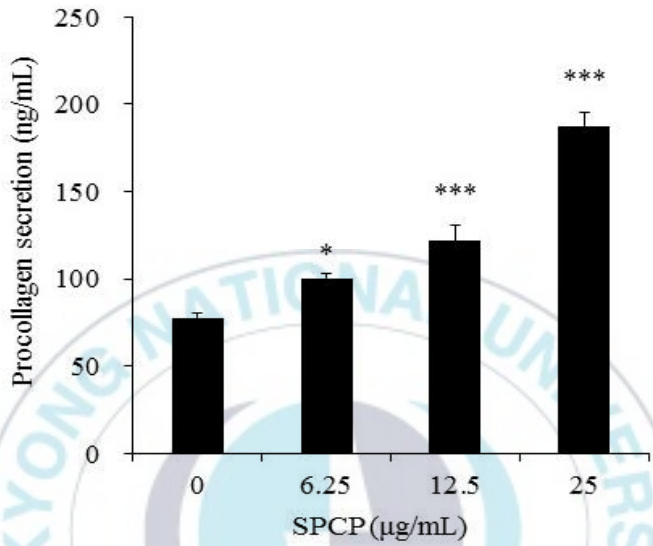

Figure 6. The treatment of SPCP induced secretion of procollagen in CCD-986sk cells. The procollagen secretion was determined by the ELISA assay following treatment with various concentrations of SPCP for 24 h. SPCP markedly increased the level of PIP in a dose-dependent manner in CCD-986sk cells. Each value represents the mean ± standard deviation of three independent experiments. * $P < 0.05$, *** $P < 0.001$ compared to the control group.

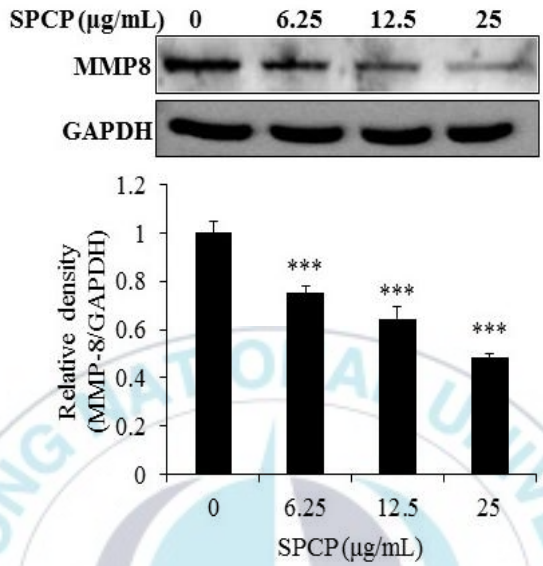

Figure 7. The treatment of SPCP decreased the expression of MMP-8 in CCD-986sk cells. The expression of MMP-8 was determined by western blot analysis following treatment with various concentrations of SPCP for 24 h. The expression level of MMP-8 protein was significantly decreased by the treatment of SPCP. Each value represents the mean ± standard deviation of three independent experiments. *** $p < 0.001$ compared to the control group.

2.5. Effect of SPCP on the migration of CCD-986sk cells

To explore the effect of SPCP on the migration of CCD-986sk cells, the wound healing assay was performed in this study. The results showed that, compared with the control, the presence of SPCP obviously promoted the migration of CCD-986sk cells (Fig. 8). This indicated that SPCP can not only promote the proliferation of CCD-986sk cells but also improve the wound healing ability. Similarly, this effect was also affected by the SPCP in a dose-dependent manner.

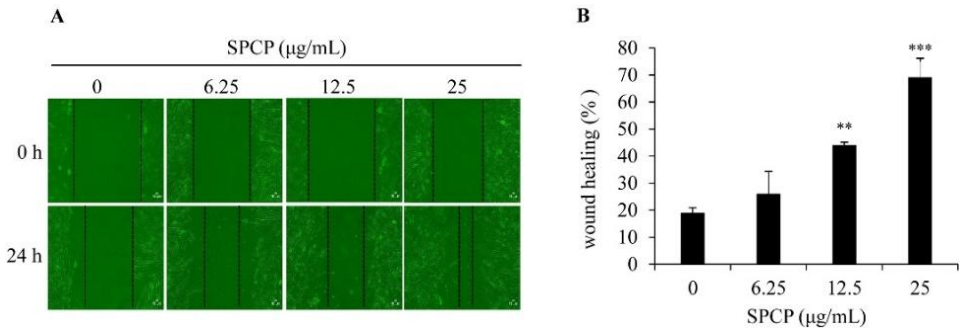

Figure 8. Treatment of SPCP enhanced repair of the scratched area. (A) A scratch wound was created by using 200 μL pipette tip in a confluent dermal fibroblast. The images were taken at 0 h and 24 h with the indicated concentration of SPCP. The dotted lines showed the area where the scratch wound was created. (B) A bar graph showed the migration of cells after 24 h following the scratch wound in cells treated with SPCP. SPCP obviously promoted the migration of CCD-986sk cells. The results are presented as the mean ± standard deviation of three independent experiments. ** $p < 0.01$, *** $p < 0.001$ compared to the control group.

2.6. Effect of SPCP on the cell cycle of CCD-986sk cells

In order to study the cell cycle of CCD-986sk cells, flow cytometry was performed. As shown in Figure 9 and Table 2, after being treated with different concentrations of SPCP, the accumulation of cells at the G_0/G_1 phase was significantly lower than that of the control group. However, the percentage of cells in S and G_2/M phases significantly increased with the treatment of SPCP. The results indicated that the presence of SPCP can transform CCD-986sk cells from G_0/G_1 phase to S and G_2/M phases. Therefore, it can be speculated that the proliferation of CCD-986sk cells was promoted by SPCP.

In order to further verify the results of cell cycle experiments, western blot analysis was performed to detect the expression levels of cell cycle related proteins, including Cdk2, Cdk4, Cdk6, cyclin D1, cyclin E, retinoblastoma protein (pRb), p21, and p27. The results showed that SPCP promoted the expression of cdk2, cdk4, cdk6, cyclin D1, cyclin E, and pRb, which are necessary for cell cycle (Fig. 10). While, the expression of p21 and p27 were decreased with the treatment of SPCP (Fig. 11), which are inhibitors of the cell cycle. Therefore, these results indicated that SPCP has a regulatory effect on the expression of cell cycle proteins. And it accelerated the cell cycle of CCD-986sk cells.

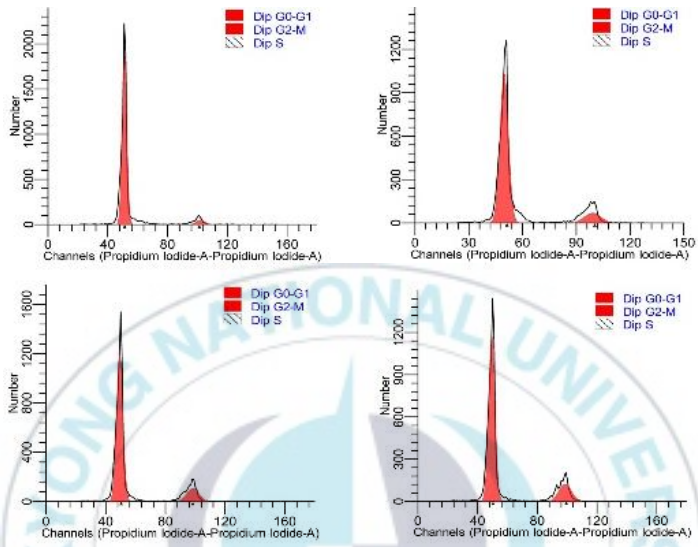

Figure 9. Treatment of SPCP promoted CCD-986sk cell cycle progression. The cell cycle of CCD-986sk was analyzed by flow cytometry following treatment with various concentrations of SPCP for 24 h. SPCP transformed CCD-986sk cells from G_0/G_1 phase to S and G_2/M phases.

Table 2. Effects of SPCP on the cell cycle of CCD-986sk cells.

SPCP (μg/mL)	G_0/G_1 (%)	S (%)	G_2/M (%)	S + G_2/M (%)
0	94.01 ± 2.494	1.84 ± 0.875	4.15 ± 1.759	5.99 ± 2.493
6.25	87.47 ± 3.604	3.51 ± 0.587 *	9.09 ± 3.500	12.6 ± 3.586 *
12.5	83.02 ± 3.647 **	3.64 ± 0.387 **	13.33 ± 1.970 **	16.98 ± 2.350 **
25	81.11 ± 2.045 **	3.73 ± 0.732 **	15.16 ± 1.339 **	18.89 ± 2.045 ***

The results are presented as the mean ± standard deviation of three independent experiments. * $p < 0.05$, ** $p < 0.01$, *** $p < 0.001$ compared to the control group.

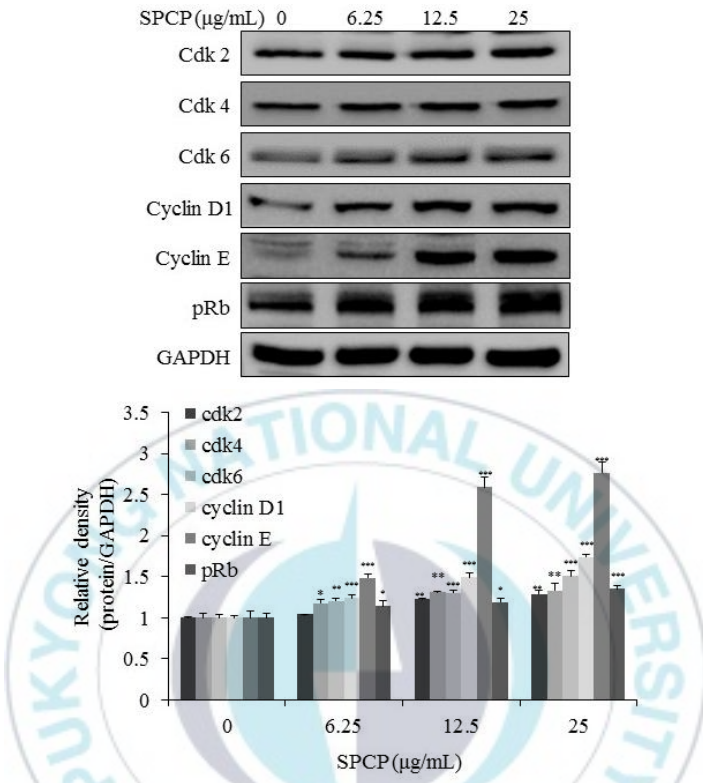

Figure 10. Treatment of SPCP decreased the expression of Cdk2, Cdk4, Cdk6, cyclin D1, cyclin E, and pRb in CCD-986sk cells. The expression levels of Cdk2, Cdk4, Cdk6, cyclin D1, cyclin E, and pRb in CCD-986sk cells were measured by western blot analysis following treatment with various concentrations of SPCP for 24 h. SPCP promoted the expression of cdk2, cdk4, cdk6, cyclin D1, cyclin E, and pRb. Each value represents the mean ± standard deviation of three independent experiments. * $p < 0.05$, ** $p < 0.01$, *** $p < 0.001$ compared to the control group.

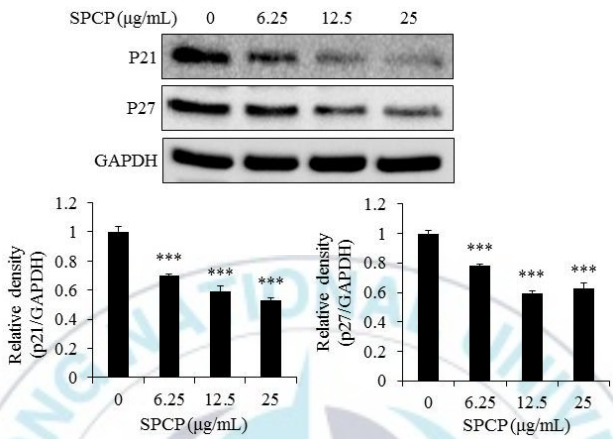

Figure 11. Treatment of SPCP regulated the expression of p21and p27 in CCD-986sk cells. The expression levels of p21and p27 in CCD-986sk cells were measured by western blot analysis following treatment with various concentrations of SPCP for 24 h. SPCP decreased the expression of p21 and p27. Each value represents the mean ± standard deviation of three independent experiments. *** $p < 0.001$ compared to the control group.

3. SPCP activated the EGFR/ERK signaling pathway in the proliferation and migration of CCD-986sk cells

3.1. Treatment of SPCP activated EGFR pathway in the CCD-986sk cells

Based on the MTS and BrdU assays, the treatment of SPCP improved the proliferation of CCD-986sk cells (Figs. 2 and 3). Thus, the effect of SPCP on the proliferation signaling pathway in CCD-986sk cells was further determined by western blot analysis. In order to determine whether EGFR was activated by the treatment of SPCP, the CCD-986sk cells were treated with different concentrations of SPCP (6.25, 12.5 and 25 μg/mL) for 24 h, respectively. The expression levels of total EGFR and p-EGFR were determined by western blot analysis. As shown in Figure 12, the phosphorylation level of EGFR was enhanced by SPCP in CCD-986sk cells, compared with control cells. Meanwhile, SPCP treatment induced the expression of essential linkers from EGFR to MAPK, including the adaptor proteins GRB2, SHC, and a guanine nucleotide exchange protein SOS (Fig. 13). These results indicated that SPCP stimulation can induce the activation of the EGFR pathway in a dose-dependent manner.

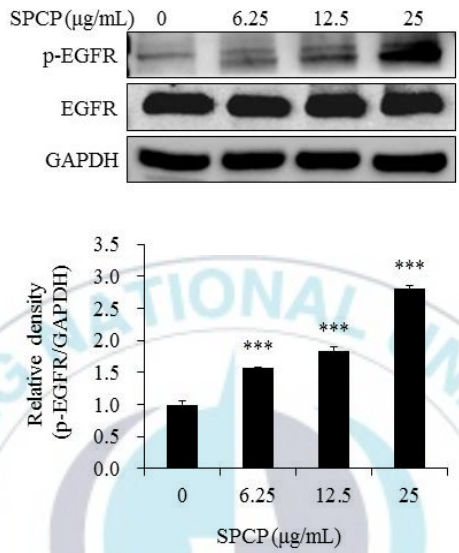

Figure 12. Treatment of SPCP enhanced the phosphorylation of EGFR in CCD-986sk cells. The phosphorylation level of EGFR in CCD-986sk cells was measured by western blot analysis following treatment with various concentrations of SPCP for 24 h. The phosphorylation level of EGFR was enhanced by the treatment of SPCP. Each value represents the mean ± standard deviation of three independent experiments. *** $p < 0.001$ compared to the control group.

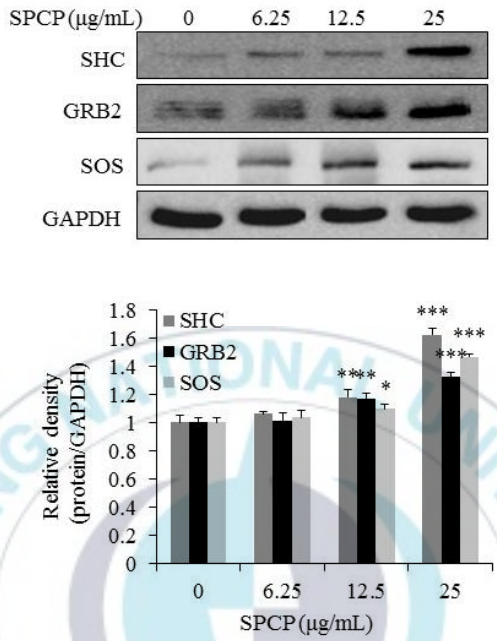

Figure 13. Treatment of SPCP enhanced the expression levels of SHC, GRB2, and SOS in CCD-986sk cells. The expression levels of SHC, GRB2, and SOS in CCD-986sk cells were measured by western blot analysis following treatment with various concentrations of SPCP for 24 h. SPCP induced the expression of SHC, GRB2, and SOS. Each value represents the mean ± standard deviation of three independent experiments. * $p < 0.05$, ** $p < 0.01$, *** $p < 0.001$ compared to the control group.

3.2. Treatment of SPCP activated Ras-MAPK pathway in the CCD-986sk cells

In order to explore whether activated EGFR induced the activation of downstream signaling, the expression level of Ras was determined by western blot analysis. As shown in Figure 14, SPCP enhanced the expression level of Ras. Ultimately, the enhanced Ras levels resulted in the phosphorylation and activation of Raf, MEK, and ERK in a dose-dependent manner (Fig. 15). These results indicated that SPCP stimulated CCD-986sk cells proliferation by activating the EGFR/MAPK/ERK signaling pathway.

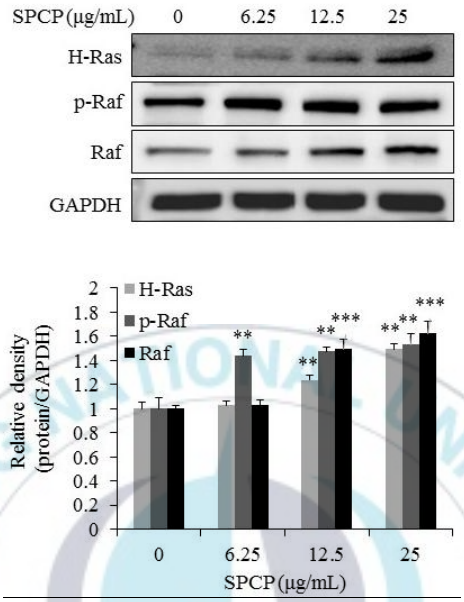

Figure 14. Treatment of SPCP enhanced the level of Ras and Raf in CCD-986sk cells. The expression level of Ras and the phosphorylated level of Raf in CCD-986sk cells were measured by western blot analysis following treatment with various concentrations of SPCP for 24 h. SPCP enhanced the expression level of Ras and p-Raf. Each value represents the mean ± standard deviation of three independent experiments. ** $p < 0.005$, *** $p < 0.001$ compared to the control group.

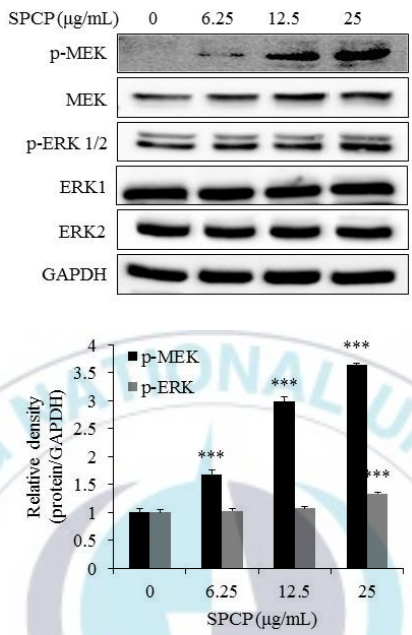

Figure 15. Treatment of SPCP enhanced the phosphorylation levels of MEK and ERK in CCD-986sk cells. The phosphorylation levels of MEK and ERK in CCD-986sk cells were measured by western blot analysis following treatment with various concentrations of SPCP for 24 h. SPCP increased the phosphorylation level of MEK and ERK. Each value represents the mean ± standard deviation of three independent experiments. *** $p < 0.001$ compared to the control group.

3.3. Inhibition of ERK reduced SPCP-induced proliferation and migration of CCD-986sk cells

In order to further determine the promotion effect of SPCP on the proliferation and migration of CCD-986sk cells via ERK signaling. U0126 was used as an inhibitor of ERK. To prove this hypothesis, the cells were pretreated with 10 μmol/L of U0126 for 1 h. Western blot analysis was performed to detect and analyze the phosphorylated level of ERK. As shown in Figure 16, the level of p-ERK was significantly enhanced by SPCP in CCD-986sk cells. However, the expression level of p-ERK decreased significantly in the SPCP-treated CCD-986sk cells which were pretreated with the inhibitor U0126.

Then, the effect of U0126 on SPCP-induced cell proliferation was studied by MTS assay and BrdU assay. As shown in Figures 17 and 18, compared with the control group, the cell proliferation was enhanced with the treatment of 25 μg/mL SPCP. However, this increase was blocked by the pretreatment of U0126. The results indicated that SPCP-induced cell proliferation was inhibited by U0126.

Moreover, in order to determine whether the effect of SPCP on the migration of CCD-986sk cells via the ERK signaling pathway, wound healing assay was performed. As shown in Figure 19, after the treatment of U0126, the migration of CCD-986sk cells was significantly reduced in the SPCP-treated group. This result indicated that the cell migration induced by SPCP was blocked by U0126.

Taken together, these results demonstrated that EGFR/ERK signaling pathway was involved in the SPCP-promoted proliferation and migration in CCD-986sk cells.

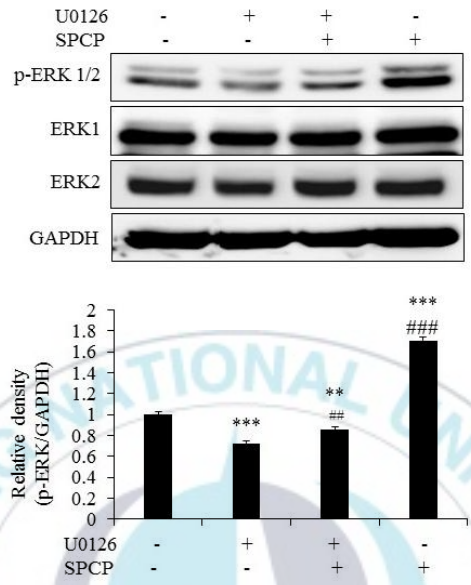

Figure 16. ERK inhibitor U0126 inhibited the level of phospho-ERK. The phosphorylation level of ERK in CCD-986sk cells was measured by western blot analysis following treatment with various concentrations of SPCP for 24 h. The phosphorylation of ERK induced by SPCP was blocked by U0126. Each value represents the mean ± standard deviation of three independent experiments. ** $p < 0.01$, *** $p < 0.001$ compared with control group. ## $p < 0.01$, ### $p < 0.001$ compared with inhibitor group.

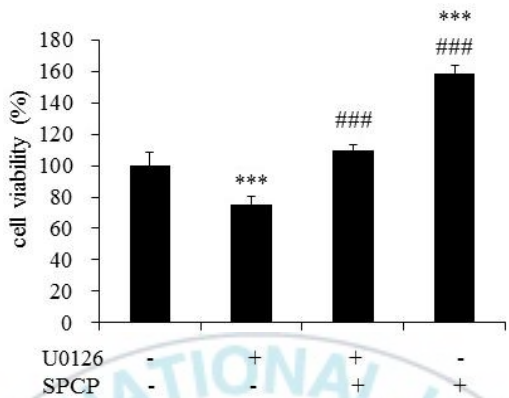

Figure 17. ERK inhibitor U0126 inhibited the viability of CCD-986sk cells. The viability of CCD-986sk cells was measured by MTS assay following treatment with various concentrations of SPCP for 24 h. The cell viability induced by SPCP was blocked by U0126. Each value represents the mean ± standard deviation of three independent experiments. *** $p < 0.001$ compared with control group. ### $p < 0.001$ compared with inhibitor group.

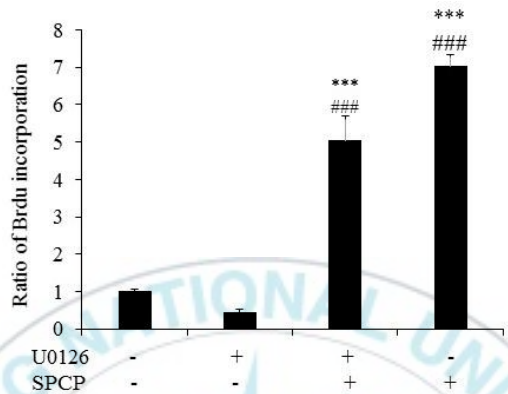

Figure 18. ERK inhibitor U0126 inhibited the proliferation of CCD-986sk cells.

The proliferation of CCD-986sk cells was measured by BrdU assay following treatment with various concentrations of SPCP for 24 h. The cell proliferation induced by SPCP was blocked by U0126. Each value represents the mean ± standard deviation of three independent experiments. *** $p < 0.001$ compared with control group. ### $p < 0.001$ compared with inhibitor group.

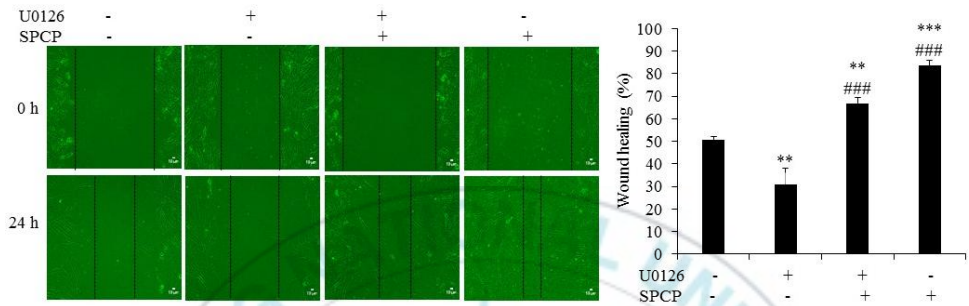

Figure 19. ERK inhibitor U0126 inhibited the migration of CCD-986sk cells. The migration of CCD-986sk cells was measured by wound healing assay following treatment with various concentrations of SPCP for 24 h. Each value represents the mean ± standard deviation of three independent experiments. The cell migration induced by SPCP was blocked by U0126. ** $p < 0.01$, *** $p < 0.001$ compared with control group. ### $p < 0.001$ compared with inhibitor group.

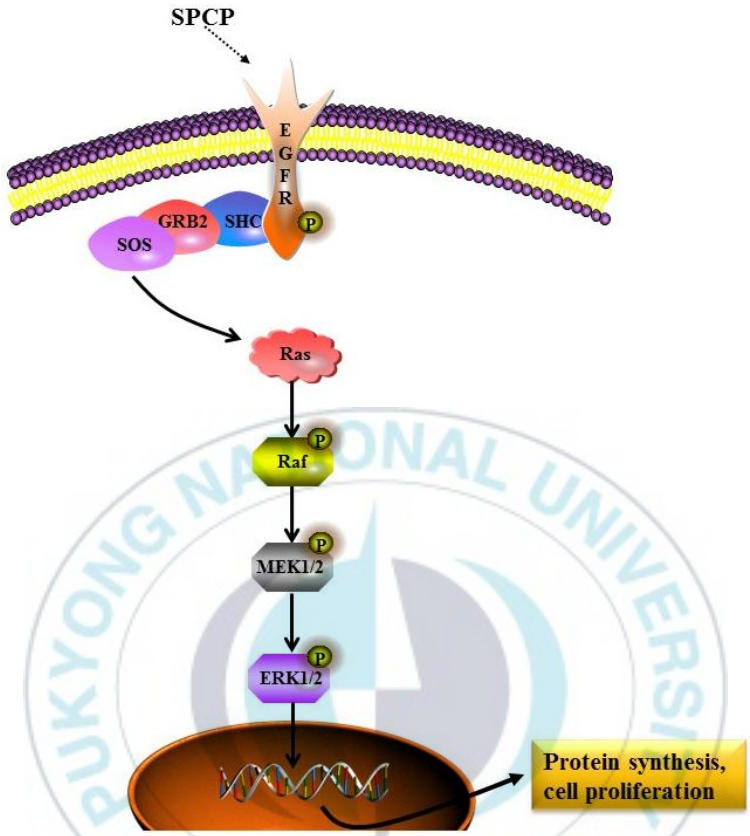

Figure 20. SPCP promoted the proliferation of CCD-986sk cells by ERFR/ERK signaling pathway.

4. SPCP activated the PI3K/Akt signaling pathway in the proliferation and migration of CCD-986sk cells

4.1. Treatment of SPCP activated PI3K/Akt signaling pathway in the CCD-986sk cells

To determine whether SPCP regulated cell cycle progression and promoted cell proliferation via PI3K/Akt signaling pathway, western blot analysis was performed. According to previous literature reports, PI3K is composed of two parts. It includes regulatory subunits and catalytic subunits, expressed by *p85* and *p110*, respectively. The results showed that the expression levels of phosphorylated p85α and p110 in CCD-986sk cells were increased after SPCP treatment compared with the control group (Fig. 21A). In addition, as shown in Figure 21B, the phosphorylated level of Akt also increased in the presence of SPCP. As is known, PTEN can inhibit PI3K/Akt signaling pathway. As shown in Figure 22, the expression level of PTEN in CCD-986SK cells was decreased after SPCP treatment. All the above results indicated that SPCP activated the PI3K/Akt signaling pathway. Meanwhile, it can inhibit the expression of PTEN in CCD-986sk cells.

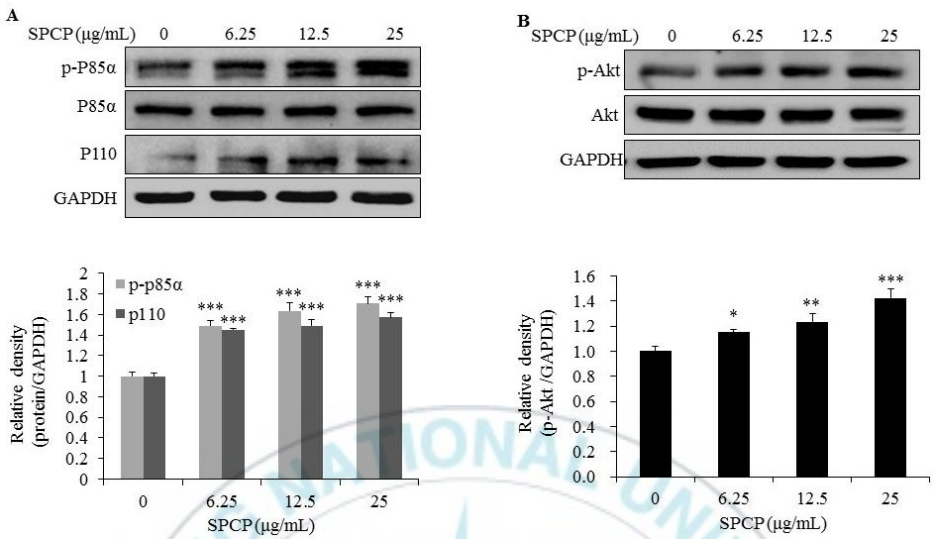

Figure 21. Treatment of SPCP enhanced the phosphorylation levels of PI3K and Akt in CCD-986sk cells. (A) The phosphorylation level of PI3K in CCD-986sk cells was measured by western blot analysis following treatment with various concentrations of SPCP for 24 h. SPCP promoted the activation of PI3K. (B) The phosphorylation level of Akt in CCD-986sk cells was measured by western blot analysis following treatment with various concentrations of SPCP for 24 h. SPCP increased the phosphorylation level of Akt. Each value represents the mean ± standard deviation of three independent experiments. * $p < 0.05$, ** $p < 0.01$, *** $p < 0.001$ compared to the control group.

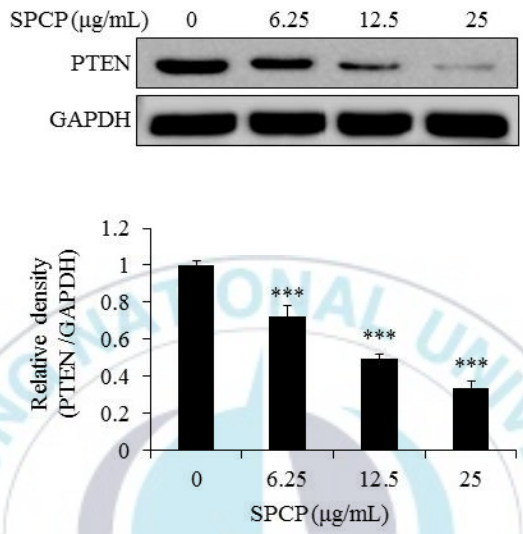

Figure 22. Treatment of SPCP reduced the expression level of PTEN in CCD-986sk cells. The expression level of PTEN in CCD-986sk cells was measured by western blot analysis. The expression level of PTEN was decreased by SPCP. Each value represents the mean ± standard deviation of three independent experiments. *** $p < 0.001$ compared to the control group.

4.2. Treatment of SPCP activated mTOR signaling pathway in the CCD-986sk cells

Akt was speculated can activate mTOR in CCD-986sk cells with SPCP treatment. To evaluate whether mTOR was activated by Akt, the phosphorylation level of mTOR was determined by western blot analysis. The results showed that the phosphorylation level of mTOR was increased with the treatment of SPCP in CCD-986sk cells compared with the control group (Fig. 23). Then, downstream signals of mTOR were further determined. As shown in Figure 24, the levels of phospho-eukaryotic translation initiation factor 4E (eIF4E)-binding protein 1 (4E-BP1) and phospho-p70 ribosomal protein S6 kinase (p70S6K) were increased with the treatment of SPCP in CCD-986sk cells.

Previous studies have shown that phosphorylation of 4E-BP1 can disrupt the complex between 4E-BP1 and the translation factor eIF4E (Ruoff *et al.*, 2016). Therefore, we determined the expression level of eIF4E. As shown in Figure 23, the expression level of eIF4E in CCD-986sk cells was not affected by SPCP treatment. However, the expression level of eIF4E in cytoplasm was inhibited, as shown in Figure 24. Meanwhile, the expression level of eIF4E was increased in nucleus with the treatment of different concentrations of SPCP in CCD-986sk cells. Combined with these results, we believed that the phosphorylation of Akt can activate mTOR. It can also enhance the phosphorylation level of p70S6K and 4E-BP1. In addition, the phosphorylation of 4E-BP1 can release eIF4E. These released eIF4E are then transferred to the nucleus.

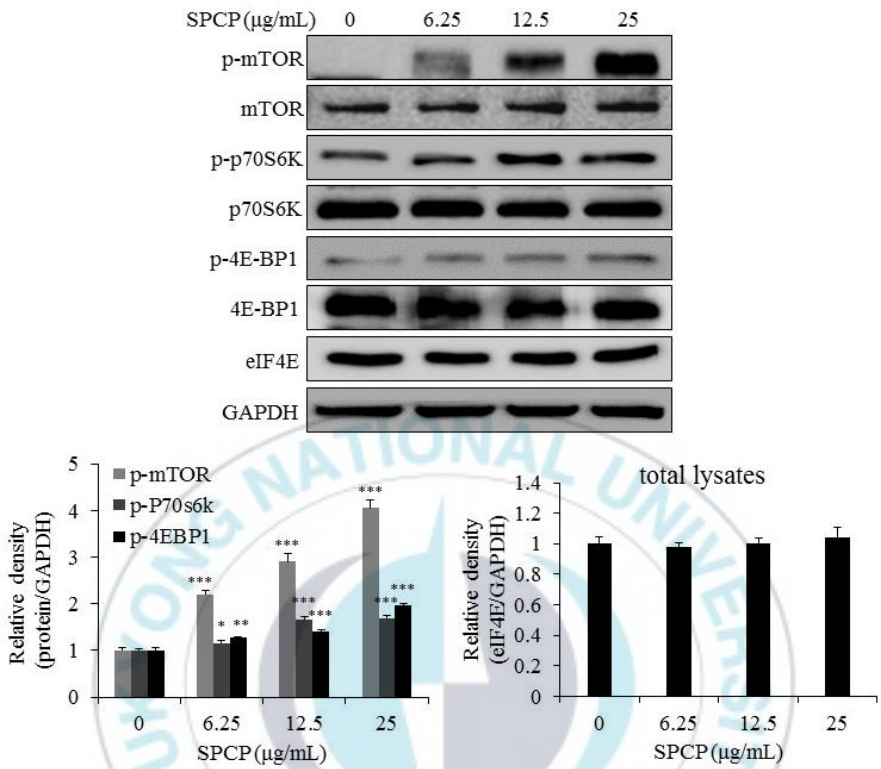

Figure 23. Effect of SPCP on the phosphorylation levels of mTOR, p70S6K, and 4E-BP1 and protein expression level of eIF4E in CCD-986sk cells. The phosphorylation levels of mTOR, p70S6K, and 4E-BP1 and protein expression level of eIF4E in CCD-986sk cells were measured by western blot analysis following treatment with various concentrations of SPCP for 24 h. The phosphorylation levels of mTOR, p70S6K, and 4E-BP1 was increased and the expression level of eIF4E was not affected by the treatment of SPCP. Each value represents the mean ± standard deviation of three independent experiments. * $p < 0.05$, ** $p < 0.001$, *** $p < 0.001$ compared to the control group.

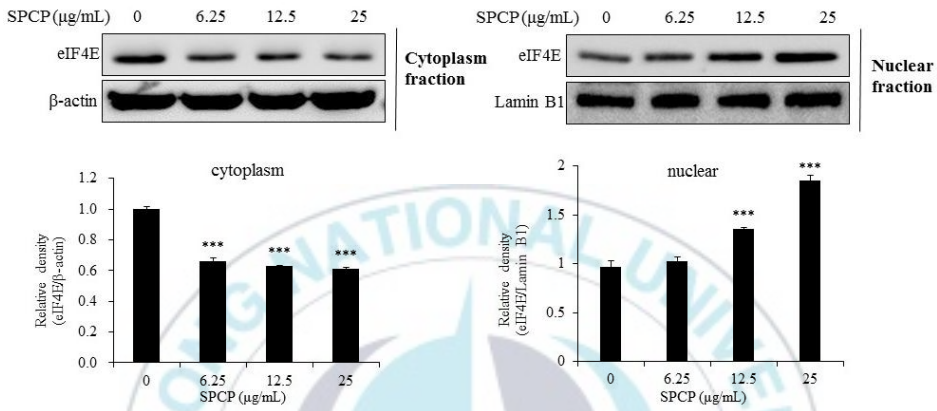

Figure 24. Effect of SPCP on translocation of eIF4E in CCD-986sk cells. The protein levels of eIF4E cytoplasm and nuclear in CCD-986sk cells were measured by western blot analysis following treatment with various concentrations of SPCP for 24 h. The expression level of eIF4E was increased in nucleus with the treatment of SPCP. Each value represents the mean ± standard deviation of three independent experiments. *** $p < 0.001$ compared to the control group.

4.3. Treatment of SPCP increased the phosphorylation of glycogen synthase kinase 3 beta (GSK3β) in the CCD-986sk cells

To further determine whether GSK3β was regulated by Akt with the treatment of SPCP in CCD-986sk cells. The phosphorylation level of GSK3β was determined by western blot analysis. As shown in Figure 25, the phosphorylation level of GSK3β was obviously promoted by SPCP. On the other hand, the treatment of SPCP enhanced the level of β-catenin in CCD-986sk cells. Therefore, we concluded that GSK3β was inactivated by the activation of Akt, which enhanced the level of β-catenin.

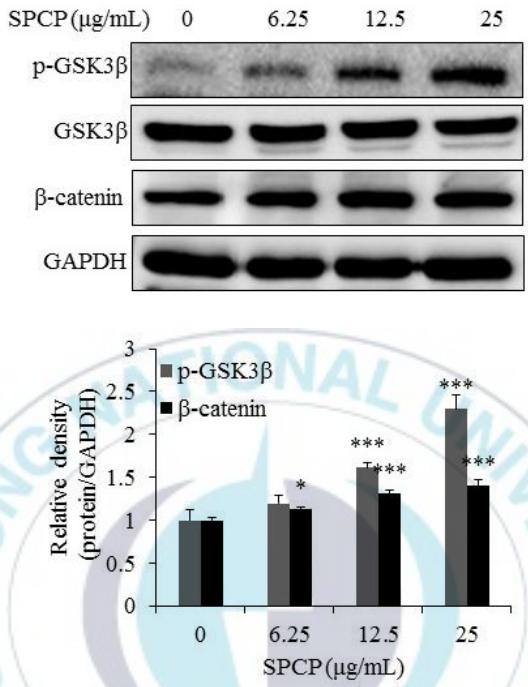

Figure 25. Effect of SPCP on the phosphorylation level of GSK3β and protein expression level of β-catenin in CCD-986sk cells. The phosphorylation level of GSK3β and protein expression level of β-catenin in CCD-986sk cells were measured by western blot analysis following treatment with various concentrations of SPCP for 24 h. The phosphorylation level of GSK3β and expression level of β-catenin were increased by the treatment of SPCP. Each value represents the mean ± standard deviation of three independent experiments. * $p < 0.05$, *** $p < 0.001$ compared to the control group.

4.4. Inhibition of PI3K reduced SPCP-induced proliferation and migration of CCD-986sk cells

In order to further determine the promotion effect of SPCP on the proliferation and migration of CCD-986sk cells via PI3K/Akt signaling, PI3K inhibitor LY294002 (50 μmol/L) was used to pretreat the cells for 1 h. Western blot analysis was used to detect and analyze the phosphorylated level of Akt. As shown in Figure 26, the level of p-Akt was significantly enhanced by SPCP in CCD-986sk cells. However, the expression level of p-Akt decreased significantly in the SPCP-treated CCD-986sk cells which were pretreated with the inhibitor LY294002.

Then, the effect of LY294002 on SPCP-induced cell proliferation was studied by MTS assay and BrdU assay. As shown in Figures 27 and 28, compared with the control group, the cell proliferation was enhanced with the treatment of 25 μg/mL SPCP. However, this increase was blocked by the pretreatment of LY294002. The results indicated that SPCP-induced cell proliferation was inhibited by LY294002.

Moreover, in order to determine whether the effect of SPCP on the migration of CCD-986sk cells via PI3K/Akt signaling pathway, wound healing assay was performed. As shown in Figure 29, after the treatment of LY294002, the migration of CCD-986sk cells was significantly reduced in the SPCP-treated group. This result indicated that the cell migration induced by SPCP was blocked by LY294002.

Taken together, these results demonstrated that PI3K/Akt signaling pathway was involved in the SPCP-promoted proliferation and migration in CCD-986sk cells.

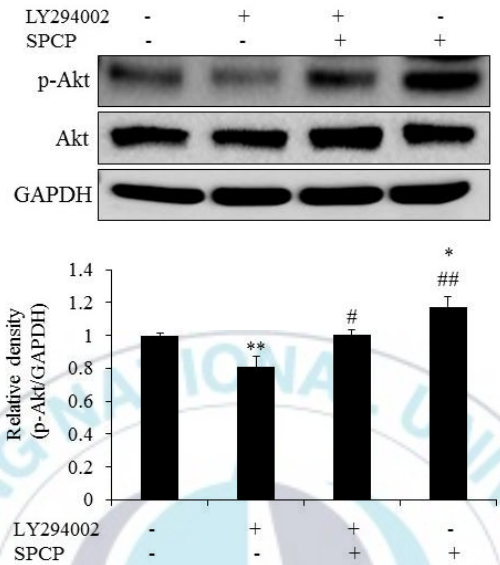

Figure 26. PI3K inhibitor LY294002 inhibited the level of phospho-Akt. CCD-986sk cells were pretreated with PI3K inhibitor LY294002 (50 μmol/L) for 1 h. The phosphorylation level of Akt in CCD-986sk cells was measured by western blot analysis following treatment with various concentrations of SPCP for 24 h. The phosphorylation level of Akt induced by SPCP was blocked by LY294002. Each value represents the mean ± standard deviation of three independent experiments. * $p < 0.05$, ** $p < 0.01$ compared with control group. $^{\#}$ $p < 0.05$, $^{\#\#}$ $p < 0.01$ compared with inhibitor group.

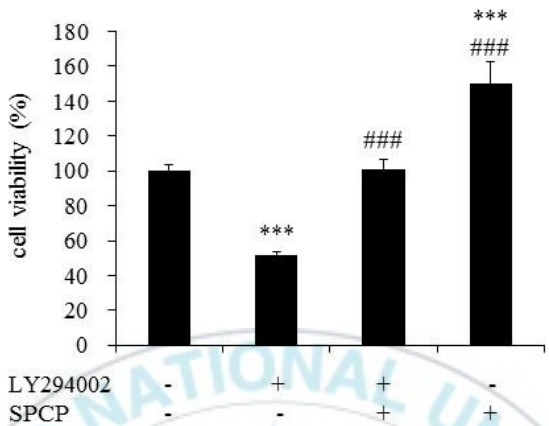

Figure 27. PI3K inhibitor LY294002 inhibited the viability of CCD-986sk cells. CCD-986sk cells were pretreated with PI3K inhibitor LY294002 (50 μmol/L) for 1 h. The viability of CCD-986sk cells was measured by MTS assay following treatment with various concentrations of SPCP for 24 h. The cell viability of CCD-986sk cells induced by SPCP was blocked by LY294002. Each value represents the mean ± standard deviation of three independent experiments. *** $p < 0.001$ compared with control group. ### $p < 0.001$ compared with inhibitor group.

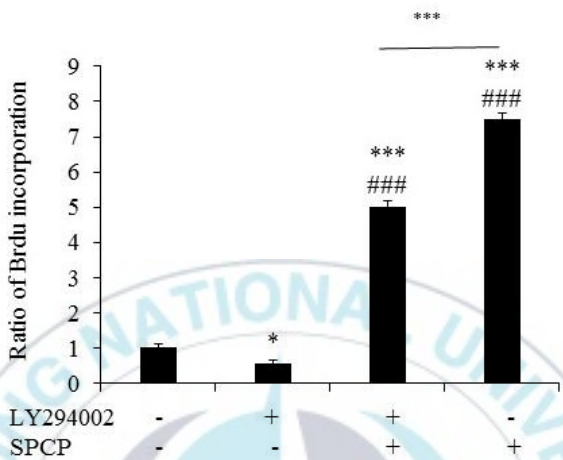

Figure 28. PI3K inhibitor LY294002 inhibited the proliferation of CCD-986sk cells. CCD-986sk cells were pretreated with PI3K inhibitor LY294002 (50 μmol/L) for 1 h. The proliferation of CCD-986sk cells was measured by BrdU assay following treatment with various concentrations of SPCP for 24 h. The proliferation of CCD-986sk cells induced by SPCP was blocked by LY294002. Each value represents the mean ± standard deviation of three independent experiments. * $p < 0.05$, *** $p < 0.001$ compared with control group. $^{###}p < 0.001$ compared with inhibitor group.

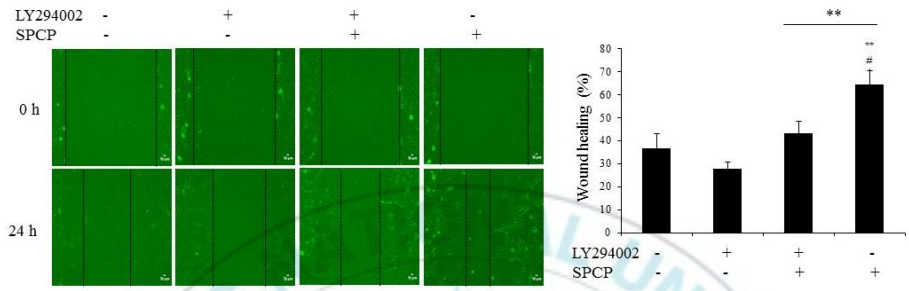

Figure 29. PI3K inhibitor LY294002 inhibited the migration of CCD-986sk cells.

CCD-986sk cells were pretreated with PI3K inhibitor LY294002 (50 μmol/L) for 1 h. The migration of CCD-986sk cells was measured by wound healing assay following treatment with various concentrations of SPCP for 24 h. The migration of CCD-986sk cells induced by SPCP was blocked by LY294002. Each value represents the mean ± standard deviation of three independent experiments. ** $p < 0.01$ compared with control group. $^{\#}$ $p < 0.05$ compared with inhibitor group.

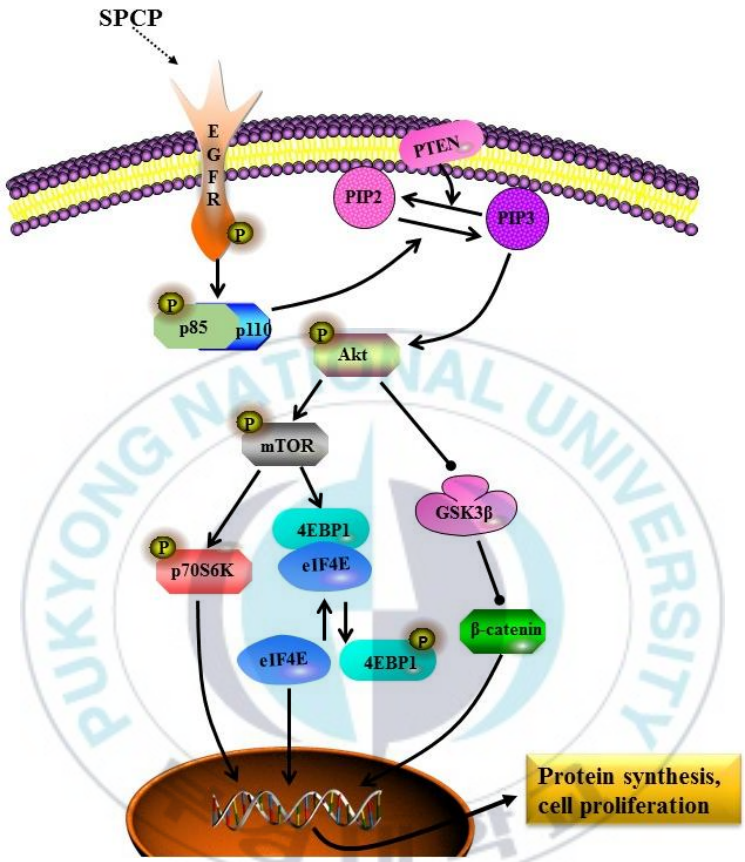

Figure 30. SPCP promoted the proliferation of CCD-986sk cells by PI3K/Akt signaling pathway.

4.5. Discussion

It has been reported that microalgal protein represents one of the most promising protein sources from food, due to their abundant and balanced amino acid composition (Becker, 2007; Brown *et al.*, 1997; Chew *et al.*, 2017). *Spirulina* (*Arthrospira*) *platensis*, an edible, photosynthetic, spiral-shaped, multicellular blue-green alga, possesses anticancer, anti-inflammatory and antioxidant effects (Belay *et al.*, 1996; El-Tantawy, 2016; Wu *et al.*, 2016). We screened suitable concentrations of SPCP according to our preliminary experimental results. The MTS assay showed that SPCP promoted the viability of human fibroblasts in a dose-dependent manner. There were 18%, 33% and 42% increases in cell proliferation over the control at 6.25, 12.5, 25 and 50 μg/mL of SPCP, respectively. Meanwhile, the BrdU assay showed that the treatment of SPCP enhanced the proliferation of CCD-986sk cells.

Dermal fibroblasts are the primary cell type responsible for the production, maintenance, and remodeling of the ECM in human skin (Meinke *et al.*, 2017; Sanchez *et al.*, 2018). Skin fibrosis is caused by an imbalance between the generation and degradation of ECM proteins, which results in a severe alteration of the skin connective tissue (Jeon *et al.*, 2010; Mac Neil, 1994; Yang *et al.*, 2011). Elastin is an integral ECM protein that accounts for 4% of the dermis and contributes to the elasticity of the skin. In neutrophil granulocytes, elastin is degraded by elastase, which is a non-specific hydrolytic enzyme capable of degrading the matrix protein collagen (Meinke *et al.*, 2017). Various structural and functional proteins deposited in the wound, such as collagen and fibronectin, are degraded by elastase. Elastase can also degrade key growth factors (such as TNF-α and TGF-β). Therefore, the accumulation of elastase can delay wound healing (Ashcroft *et al.*, 2000; Wiegand *et al*., 2011). In this study, the activity of elastase was also examined and we found

that treatment with the SPCP inhibited the activity of elastase in CCD-986sk cells. The activity of elastase was reduced in a dose-dependent manner, with a maximum decrease of 32% compared to the control (untreated cells) treated with 25 μg/mL of the SPCP. Type I collagen is the major structural protein of skin connective tissue, providing strength and flexibility to the skin (Tracy *et al.*, 2016; Gonzalez *et al.*, 2016). PIP, a soluble precursor to type I collagen, is secreted from fibroblasts within the dermis, and subsequently proteolytically cleaved to form insoluble collagen fibers (Salsasescat *et al.*, 2010; Shoulders and Raines, 2010). In this study, cell collagen production was induced by SPCP, which was 30-142% higher than the control group. On the other hand, collagenases are a subfamily of the matrix MMP family and are capable of cleaving collagen (Kawatani *et al.*, 2015). MMP-8, a kind of collagenases, is widely present in the connective tissue of most mammals (Hoseini *et al.*, 2015; Zhang *et al.*, 2013). Meanwhile, MMP-8 serves as a key enzyme in the degradation of collagen and stimulates the degradation of other major dermal components (Herman *et al.*, 2001). In this study, the expression level of MMP-8 was significantly decreased by the treatment of SPCP in a dose-dependent manner. Thus, the increase in collagen might be due to a decrease in the expression of MMP-8.

Previous studies have shown that substances extracted from spirulina can effectively promote wound healing (Gunes *et al.*, 2017; Syarina *et al.*, 2015). Some researchers have studied the effect of its extract on rat fibroblasts. The results showed that spirulina extract could not only maintain cell viability but also improve its proliferation (Jung *et al.*, 2013). In addition, it is reported that spirulina extract, which combined with silk sericin, has the ability to promote wound healing. This therapeutic effect resulted in the proliferation of human skin fibroblasts due to the water extract from *Spirulina platensis* (Bari *et al.*, 2017). In our studies, from the

analysis of the data, we can find that SPCP can significantly improve the proliferation and migration of CCD-986sk cells. In addition, the proliferation of dermal fibroblasts is one of the important factors for skin wound healing (Woodley, 2017). An important factor to control cell proliferation is the interface between the cell cycle signaling system and the growth factor signaling pathway. (Ponnusamy *et al.*, 2017; Sears and Nevins, 2002). Thus, the cell cycle was analyzed by flow cytometry. From the results, we can see that the difference between the control group and the SPCP-treated group was that the proportion of G_0/G_1 cells was significantly reduced under the treatment of SPCP. On the other hand, SPCP treatment can increase the number of cells in S phase and G_2/M phase. Therefore, we concluded that SPCP can effectively transform cells from G_0/G_1 phase to S phase and G_2/M phase. Thus, SPCP promoted the proliferation of CCD-986sk cells by promoting the cell cycle transfer to S and G_2/M phases from the G_0/G_1 phase.

Previous studies have shown that the cell cycle is regulated by a variety of signaling systems (Duronio and Yue, 2013). In this study, western blot analysis was used to determine the expression levels of cell cycle related proteins in CCD-986sk cells. These proteins include cyclin D, cyclin E, Cdk2, Cdk4, Cdk6 and pRb. In addition, the expression levels of p21 and p27 were also determined, which were inhibitors of the cell cycle (Coqueret, 2003). The results showed that the expression levels of cyclin D, cyclin E, Cdk2, Cdk4, Cdk6, and pRb were increased with the treatment of SPCP. Meanwhile, the expression levels of p21 and p27 were inhibited after SPCP treatment. Previous studies have shown that proliferation signaling pathways have a regulatory effect on cell cycle. Cyclins are the primary targets (van den Heuvel and Harlow, 1993). Cyclin D can not only interact with Cdk4 to form complex but also with Cdk6 to form complex. Similarly, cyclin E can bind with Cdk2

to form an active complex. These complexes can effectively control the changes of G_1 phase and DNA synthesis. So, they can be used to regulate cell cycle (Bertoli *et al.*, 2013; Besson *et al.*, 2008; Sheaff *et al.*, 1997). From the results, we can see that SPCP promotes the cell cycle of CCD-986sk cells by promoting the cell cycle transition from G_0/G_1 phase to S and G_2/M phase and regulating the expression levels of related proteins that affect the cell cycle.

The MTS assay and BrdU assay demonstrated that SPCP promoted the proliferation of CCD-986sk cells. It was reported that the activation of EGFR serves an important role in cell proliferation, which (Baker, 2001; Jin *et al.*, 2015). Zhang and Liu, 2002). In this study, the phosphorylation level of EGFR was increased in SPCP-treated cells, compared with control cells. Additionally, the expression levels of essential linkers from EGFR to MAPK, which include adaptor protein GRB2, SHC, and SOS (Liang *et al.*, 2018), were induced by the SPCP treatment in a dose-dependent manner. These data indicated that the EGFR pathway was activated by SPCP in a dose-dependent manner. Previous studies have shown that one of the main activated downstream signaling pathways is the Ras/Raf/MEK/ERK1/2 pathway, which controls proliferation and differentiation (Corcoran *et al.*, 2012; D'Ambrosio *et al.*, 2011; Herbst, 2004; Jutten and rouschop, 2014; Stewart *et al.*, 2015). We, therefore, detected the activation of this downstream signaling pathway, finding that the expression level of Ras increased after SPCP treatment. This then led to the phosphorylation and activation of Raf, MEK, and ERK in a dose-dependent manner. The phosphorylation of ERK results in the activation of its kinase activity and leads to phosphorylation of its many downstream targets, which are involved in the regulation of cell proliferation (Schevzov *et al.*, 2015). Meanwhile, MTS assay and BrdU assay showed that SPCP-induced proliferation of CCD-986sk cells was

inhibited by ERK inhibitor U0126. Otherwise, the migration of CCD-986sk cells induced by SPCP was also inhibited by ERK inhibitor U0126. These results suggest that SPCP plays an important role in the phosphorylation and activation of ERK in promoting the proliferation and migration of CCD-986sk cells.

When EGFR is activated, the PI3K/Akt signaling pathway can be further activated. It can regulate cell cycle and promote cell proliferation (Li *et al.*, 2014; Liu *et al.*, 2017; Wu *et al.*, 2017). Then, the activated PI3K/Akt signaling pathway can activate downstream signals. In addition, enhanced phosphorylation of PI3K/Akt signaling pathway can promote cell proliferation (Chang *et al.*, 2003; Manikarna *et al.*, 2015; Tee and Blenis, 2005; Wang *et al.*, 2013). From our previous research, we know that the EGFR signal in CCD-986sk cells can be activated by SPCP. Therefore, we investigated whether PI3K/Akt signaling pathway was involved in the proliferation and migration in CCD-986sk cells which were induced by SPCP. The results showed that SPCP can enhance the levels of p-p85α, p110, and p-Akt in CCD-986sk cells.

PTEN is a natural inhibitor of the PI3K/Akt signaling pathway (Maehama and Dixon, 1999; Milella *et al.*, 2015; Vanhaesebroeck *et al.*, 2016). After SPCP treatment, the expression level of PTEN in CCD-986sk cells decreased. It has been reported that mTOR plays an important role in the regulation of cell proliferation and it can be activated by p-Akt (Wang *et al.*, 2015; Zhang *et al.*, 2007). 4EBP1 and p70S6K are two important phosphorylation substrates for mTOR signals (Fingar *et al.*, 2004; Lawrence and Abraham, 1997). It is well known that the regulation of translation is one of the important factors controlling cell proliferation. eIF4E plays an important role in the regulation of translation. The process of translation can be inhibited by the combination of 4EBP1 and eIF4E. When activated mTOR

phosphorylates 4EBP1, 4EBP1 releases eIF4E to promote protein synthesis (Ruoff *et al.*, 2016). In addition, another phosphorylated substrate of mTOR is p70S6K, which can also regulate translation (Laplante and Sabatini, 2009; Laplante and Sabatini, 2012). In our study, phosphorylation levels of 4EBP1 and p70S6K increased with SPCP treatment. Meanwhile, the content of eIF4E in the nucleus of CCD-986sk cells increased with the treatment of SPCP. In addition, the activity of many transcription factors is affected by β-catenin. And β-catenin can be degraded by GSK3β (Liu *et al.*, 2002; Nusse and Clevers, 2017). However, the activity of GSK3β was inhibited by p-Akt (Grimes and Jope, 2001; Park *et al.*, 2014). Thus, the β-catenin is released by inactivated GSK3β. Further, the β-catenin regulates the transcription factors and regulates the expression of various genes, including proteins that regulate cell cycle (Grimes and Jope, 2001; Valenta *et al.*, 2012). In this study, we found that the phosphorylation level of GSK3β in CCD-986sk cells was promoted by SPCP. At the same time, the expression level of β-catenin was also increased after SPCP treatment. These results suggested that in the process of SPCP-induced proliferation and migration of CCD-986sk cells, PI3K/Akt/mTOR signaling pathway played an important role. In order to further determine the role of Akt in the proliferation and migration of CCD-986sk cells promoted by SPCP, pretreatment with PI3K inhibitor LY294002 was carried out. The level of p-Akt in LY294002 pretreated cells was lower than that in SPCP treated cells. MTS assay and BrdU assay showed that the proliferation of CCD-986sk cells in SPCP-treated group was inhibited by PI3K inhibitor LY294002. Meanwhile, the migration of CCD-986sk cells induced by SPCP was also inhibited by inhibitor LY294002. These results suggested that SPCP played an important role in the phosphorylation and activation of Akt in promoting the proliferation and migration of CCD-986sk cells.

In summary, after SPCP treatment, the proliferation and migration of human dermal fibroblast CCD-986sk cells were enhanced. This can effectively promote wound healing. In this process, EGFR/ERK and PI3K/Akt signaling pathway play an important role. The results obtained in this study can support the positive role of SPCP in wound healing. In addition, we also put forward the mechanisms that SPCP plays an active role in skin wound healing.

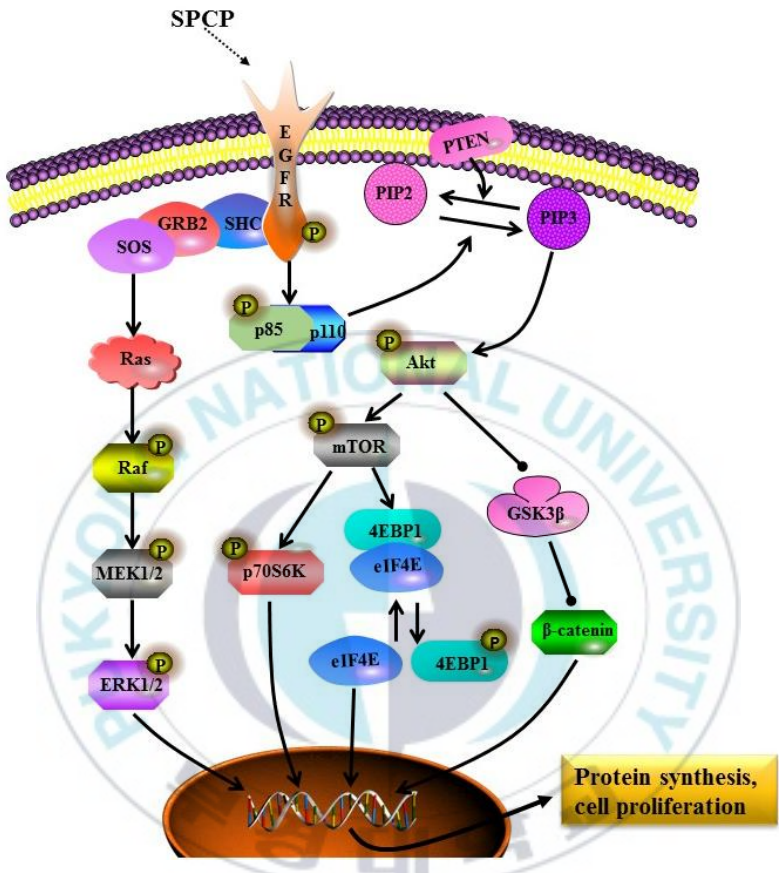

Figure 31. Effect of SPCP on the proliferation and migration of CCD-986sk cells.

5. Effect of SPCP on the skin wound healing in C57BL/6 mice

5.1. Treatment of SPCP accelerated the wound healing

In order to determine the effect of SPCP on the skin wound healing, C57BL/6 mice were used. To prove this hypothesis, we created a full thickness excisional wound mouse models. From the pictures on days 0, 3, 6 and 9, we can see that the percentage of wound closure in the mice which were treated with EGF and SPCP was higher than the mice which were treated only with Vaseline (Fig. 32).

Myofibroblasts play an important role in skin wound healing (Hinz, 2016; Plikus *et al.*, 2017). One of the myofibroblast-specific markers is α-SMA (Hinz *et al.*, 2007). Thus, the expression level of α-SMA was determined by western blot analysis. As shown in Figure 33, the expression level of α-SMA was higher in EGF and SPCP-treated groups than the control group. These results indicated that SPCP enhanced wound healing by increasing the level of myofibroblasts.

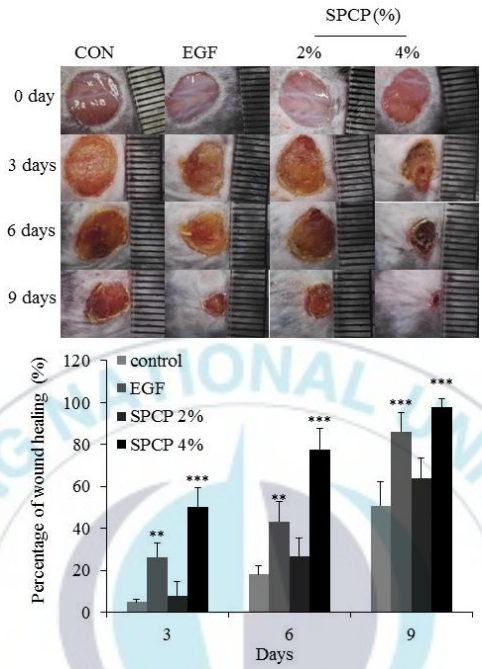

Figure 32. Treatment of SPCP enhanced the skin wound healing in C57BL/6 mice. The effect of SPCP on the skin wound healing was measured using a full thickness excisional wound model in C57BL/6 mouse. Each value represents the mean ± standard deviation of five mice. ** $p < 0.01$, *** $p < 0.001$ compared with control group.

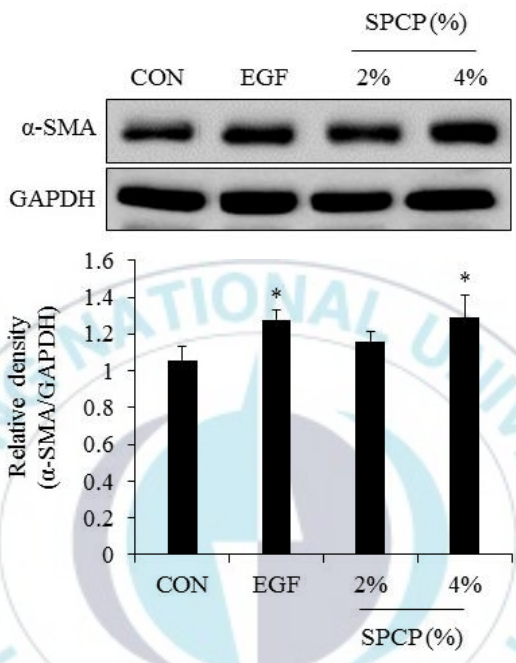

Figure 33. Treatment of SPCP induced the expression level of α-SMA in C57BL/6 mice. The expression level of α-SMA in C57BL/6 mice was measured by western blot analysis following treatment with various concentrations of SPCP for 9 days. Each value represents the mean ± standard deviation of three independent experiments. * $p < 0.05$ compared to the control group.

5.2. Effect of SPCP on the body weight of C57BL/6 mice

To determine the effect of SPCP on the body weight of C57BL/6 mice, the body weights were recorded. From the results (Table 3) we can see that the body weights of the mice in the SPCP-treated group had no difference with the mice in the control group. The results indicated that SPCP had no effect on the body weight of C57BL/6 mice.

Table 3 Effect of SCPC on the body weight of C57BL/6 mice

			SPCP (%)	
	Control	**EGF**	**2%**	**4%**
Basal BW (g)	22.86 ± 0.40	21.66 ± 0.74	23.00 ± 0.41	22.40 ± 0.35
Final BW (g)	22.92 ± 0.68	22.18 ± 0.66	23.08 ± 0.77	22.76 ± 0.58

The results are presented as the mean ± standard deviation of three independent experiments.

5.3. Effect of 9 days treatment with SPCP on lipid peroxide and antioxidant enzymes in granulation tissue homogenate

In order to determine the effect of SPCP on the activity of SOD, ELISA assay was performed using an ELISA kit. As shown in Table 4, the mice which were treated with SPCP had a higher activity of SOD, compared with the control group. Further, the activity of SOD induced by SPCP in a dose-dependent manner. These results indicated that SPCP may have a positive effect on antioxidant by enhancing the activity of SOD during the skin wound healing in mice.

In order to determine the effect of SPCP on the activity of CAT, ELISA assay was performed using an ELISA kit. As shown in Table 4, the mice which were treated with SPCP had a higher activity of CAT, compared with the control group. Further, the activity of CAT induced by SPCP in a dose-dependent manner. These results indicated that SPCP may have a positive effect on antioxidant by enhancing the activity of CAT during the skin wound healing in mice.

In order to determine the effect of SPCP on the level of MDA, ELISA assay was performed using an ELISA kit. As shown in Table 4, the mice which were treated with SPCP had a lower level of MDA, compared with the control group. These results indicated that SPCP may have a positive effect on antioxidant by inhibiting the level of MDA during skin wound healing in mice.

Table 4 Effect of 9 days treatment with SPCP on lipid peroxide and antioxidant enzymes in granulation tissue homogenate

	SOD activity (U/mg protein)	CAT activity (mU/mg protein)	MDA (nmol/mg protein)
Control	12.55 ± 0.08	3.55 ± 0.22	0.98 ± 0.04
EGF	13.59 ± 0.43*	4.65 ± 1.19	0.64 ± 0.08**
2% SPCP	13.87 ± 0.53*	4.52 ± 0.19	0.60 ± 0.06***
4% SPCP	15.61 ± 0.36***	6.02 ± 0.54**	0.36 ± 0.05***

The results are presented as the mean ± standard deviation of three independent experiments. * $p < 0.05$, ** $p < 0.01$, *** $p < 0.001$ compared to the control group.

5.4. SPCP enhanced the wound healing through ERK signaling pathway in C57BL/6 mice

According to previous results in CCD-986sk cells, we know that the EGFR/ERK signaling pathway was involved in SPCP-induced proliferation and migration of CCD-986sk cells. Thus, the effect of SPCP on the phosphorylated level of ERK was determined using western blot analysis. The results showed that the levels of p-ERK were increased with the treatment of SPCP in skin granulation tissue of C57BL/6 mice (Fig. 34). This indicated that SPCP promoted skin wound healing in C57BL/6 mice via the ERK signaling pathway.

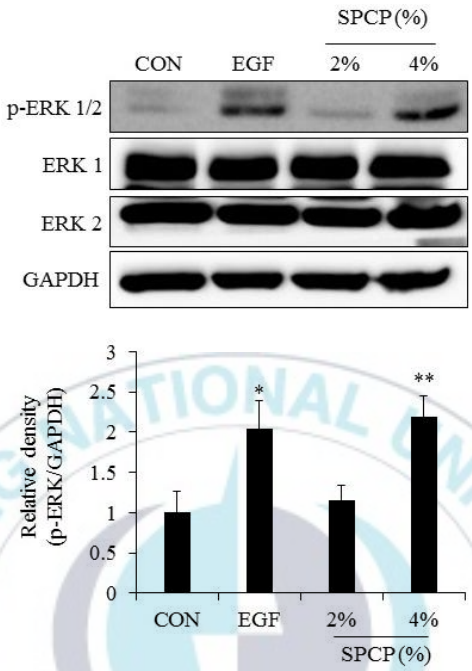

Figure 34. Treatment of SPCP enhanced the phosphorylation level of ERK in C57BL/6 mice. The phosphorylation level of ERK in C57BL/6 mice was measured by western blot analysis following treatment with various concentrations of SPCP for 9 days. The phosphorylation level of ERK was increased by SPCP. Each value represents the mean ± standard deviation of three independent experiments. * $p <$ 0.05, ** $p < 0.01$ compared to the control group.

5.5. SPCP enhanced the wound healing through Akt signaling pathway in C57BL/6 mice

According to previous results in CCD-986sk cells, we know that the PI3K/Akt signaling pathway was involved in SPCP-induced proliferation and migration of CCD-986sk cells. Thus, the effect of SPCP on the phosphorylated level of Akt was determined using western blot analysis. The results showed that the levels of p-Akt were increased with the treatment of SPCP in skin granulation tissue of C57BL/6 mice (Fig. 35). This indicated that SPCP promoted skin wound healing in C57BL/6 mice via the Akt signaling pathway.

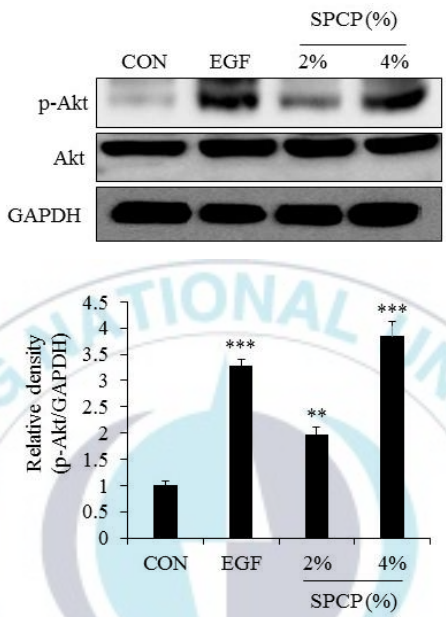

Figure 35. Treatment of SPCP enhanced the phosphorylation level of Akt in C57BL/6 mice. The phosphorylation level of Akt in C57BL/6 mice was measured by western blot analysis following treatment with various concentrations of SPCP for 9 days. The phosphorylation level of Akt was increased by SPCP. Each value represents the mean ± standard deviation of three independent experiments. ** $p < 0.01$, *** $p < 0.001$ compared to the control group.

5.6. SPCP enhanced the wound healing through TGF-β1/Smads signaling pathway

TGF-β1/Smads signal transduction pathway is a signal transduction pathway and plays an important role in tissue repair (Verrecchia and Mauviel, 2002). TGF-β1 is involved in the whole process of inflammation, proliferative phase, and plasticization during wound healing (Wu *et al.*, 2019). Thus, the effect of SPCP on the TGF-β1/Smads signaling pathway was determined using western blot analysis. The results showed that the levels of TGF-β1 were increased with the treatment of SPCP in skin granulation tissue of C57BL/6 mice (Fig. 36). Meanwhile, the level of p-Smad2 was increased with the treatment of SPCP in skin granulation tissue of C57BL/6 mice (Fig. 37). These results indicated that SPCP promoted skin wound healing in C57BL/6 mice via TGF-β1/Smads signaling pathway.

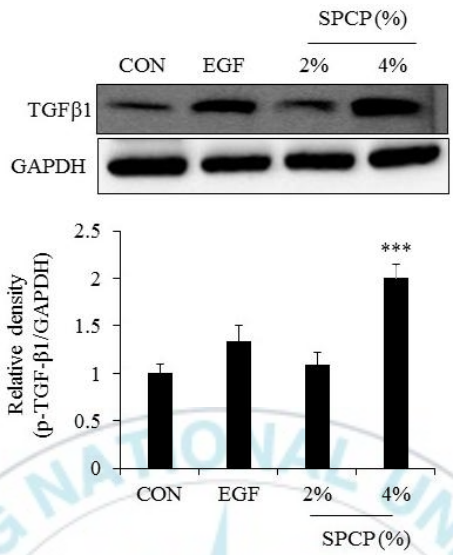

Figure 36. Treatment of SPCP enhanced the protein expression of TGF-β1 in C57BL/6 mice. The protein expression level of TGF-β1 in C57BL/6 mice was measured by western blot analysis following treatment with various concentrations of SPCP for 9 days. The expression level of TGF-β1 was increased by SPCP. Each value represents the mean ± standard deviation of three independent experiments. *** $p < 0.001$ compared to the control group.

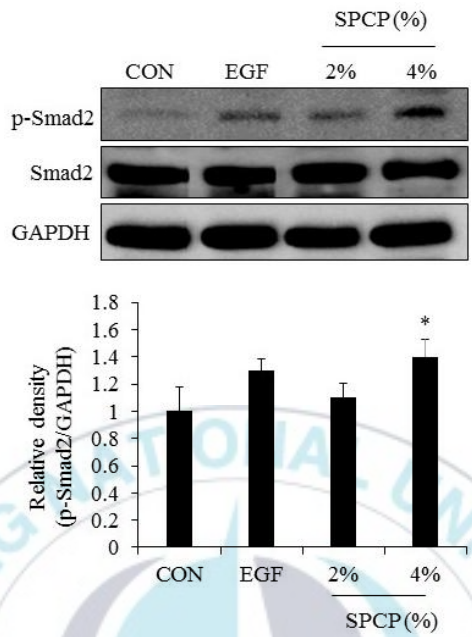

Figure 37. Treatment of SPCP enhanced the phosphorylation levels of Smad2 in C57BL/6 mice. The phosphorylation level of Smad2 in C57BL/6 mice was measured by western blot analysis following treatment with various concentrations of SPCP for 9 days. The phosphorylation level of Smad2 was increased by SPCP. Each value represents the mean ± standard deviation of three independent experiments. * $p < 0.05$ compared to the control group.

5.7. SPCP regulated the expression of collagen

In order to determine the effect of SPCP on the expression level in granulation tissue of C57BL/6 mice, western blot analysis was performed. The results showed that the expression level of type I collagen was higher in SPCP-treated group than the control group (Fig. 38). This result indicated that SPCP enhanced the expression level of type I collagen during skin wound healing.

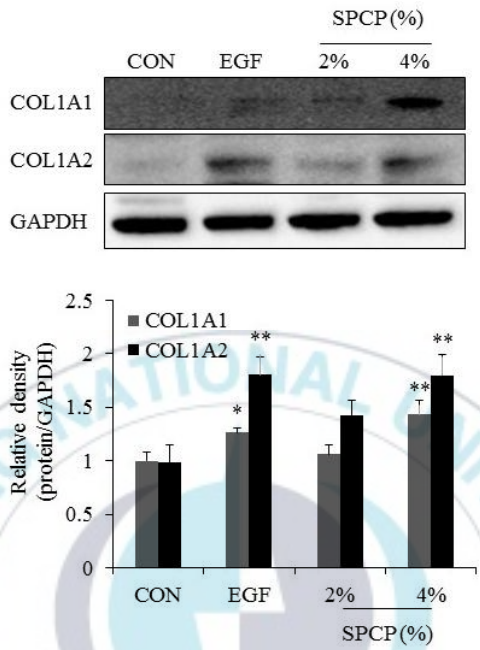

Figure 38. Treatment of SPCP enhanced the protein expression of type I collagen in C57BL/6 mice. The protein expression levels of COL1A1 and COL1A2 in C57BL/6 mice was measured by western blot analysis following treatment with various concentrations of SPCP for 9 days. The protein expression levels of COL1A1 and COL1A2 were increased by SPCP. Each value represents the mean ± standard deviation of three independent experiments. * $p < 0.05$, ** $p < 0.01$ compared to the control group.

5.8. Discussion

Normally, for the damage of the external environment, skin can protect the integrity and function of internal organs very well (Joshi *et al.*, 2016; Park *et al.*, 2015). Therefore, in the process of resisting environmental stimuli, the skin will be damaged to varying degrees. If the damage is serious, the function of internal organs will change, even death (Kim *et al.*, 2018; Zhao *et al.*, 2017). Therefore, it is very meaningful to study how to promote the efficiency of skin wound healing. As we all know, the process of wound healing is very complicated. Among them, the key factor is how to form and reconstruct new tissue cells (Pereira and Bártolo, 2016; Sorg *et al.*, 2017). According to previous studies, we know that SPCP enhanced the proliferation and migration of human fibroblasts, which play a crucial role in the formation and remodeling of new tissues. Therefore, this study was aimed to determine the effect of SPCP on the skin wound healing in C57BL/6 mice and investigate the mechanisms during this process.

In the present study, SPCP promoted skin wound healing in C57BL/6 mice. It is reported that excessive reactive oxygen species (ROS) can inhibit wound healing (Kurahashi and Fujii, 2015; Landén *et al.*, 2016). Superoxide anion free radicals (O^{2-}) are natural intermediates in various physiological reactions of organisms. It is a kind of ROS with strong oxidation ability and is one of the important factors of biological oxygen toxicity (Sailaja Rao *et al.*, 2011). SOD is a free radical scavenger, which exists widely in various tissues of organisms and can scavenge free radical O^{2-} (Nimse and Pal, 2015). CAT is an enzyme scavenger that can decompose hydrogen peroxide into water and oxygen. Hydrogen peroxide is scavenged by the CAT to protect the body from oxidative damage (Sies, 2017). Antioxidants play an important role in wound healing because they can protect the wound area from oxidative

damage (Joshi *et al.*, 2016; Ram *et al.*, 2014). Additionally, spirulina has an antioxidant defense system, which removes ROS that can damage cells by inducing oxidative stress (Bashandy *et al.*, 2016; Li-Chen *et al.*, 2005; Patil *et al.*, 2018). Thus, we evaluated the antioxidant effect of SPCP in wound healing by measuring SOD, CAT activity and MDA content. The results showed that SPCP reduced MDA content. At the same time, the activity of SOD and CAT in granulation tissue of SPCP treatment group was higher than that of the control group. These results suggested that SPCP can promote the healing of skin wounds in mice through antioxidation.

ERK1/2 can be phosphorylated by some growth factors and hydrogen peroxide, and then enter the nucleus to act on transcription factors in the nucleus, such as c-myc, c-jun, and nuclear factor kappa-light-chain-enhancer of activated B cells (NF-κB) (Meloche and Pouysségur, 2007). ERK1/2 can promote the activity of downstream genes, affect the transcription and expression of downstream genes, regulate various functions of cells, such as metabolism and survival, and ultimately affect the corresponding biology of cells (He *et al.*, 2008). Only phosphorylated ERK1/2 has active (Mebratu and Tesfaigzi, 2009). Previous studies showed that SPCP increased the phosphorylation level of ERK1/2. Thus, the expression level of p-ERK1/2 in granulation tissue of C57BL/6 mice was determined by western blot analysis. The results showed that SPCP activated ERK1/2 signal in skin granulation tissue of C57BL/6 mice. In addition, PI3K/Akt signaling pathway, as one of the more common signaling pathways *in vivo*, is involved in regulating various cell activities, such as cell inflammation, proliferation and differentiation (Coutant *et al.*, 2002). PI3K/Akt pathway integrates signals from growth factors and cytokines and transmits these signals through multiple downstream effectors (Engelman *et al.*, 2006). In turn, these effectors regulate basic cellular functions, including growth,

metabolism, survival, and proliferation (Kornasio *et al.*, 2009). Previous studies have found that SPCP activates the PI3K/Akt signaling pathway in CCD-986sk cells. Therefore, we examined the activation of the Akt signal in SPCP-induced mouse skin wound healing. The results showed that SPCP activated Akt signal in skin granulation tissue of C57BL/6 mice.

In the process of wound healing, wound contraction and ECM recombination are very important (Schultz and Wysocki, 2009). In the process of wound contraction, one of the most important factors is the expression and differentiation of myofibroblasts. The expression of α-SMA is an important marker of myofibroblasts (Hinz, 2007). Previous studies have shown that in the process of fibroblast differentiation into myofibroblasts, the stimulation of TGF-β on wounds is very important (Bochaton-Piallat *et al.*, 2016; Chin *et al.*, 2004). In this study, on the 9th day after the injury, SPCP treatment significantly increased the expression of TGF-β1 in mice. Meanwhile, on the 9th day of wound healing, the expression of α-SMA in granulation tissue of SPCP treated mice was significantly higher than that of the control group. Meanwhile, the phosphorylation level of Smad2, which is the downstream signal of TGF-β1, was enhanced by the treatment of SPCP in granulation tissue in C57BL/6 mice. These results suggest that SPCP promotes skin wound healing in mice by activation TGF-β1/Smad signaling pathway and increasing the expression of α-SMA. The ECM of the dermis consists of collagen and is produced by fibroblasts (Tracy *et al.*, 2014). In particular, type I collagen is the most prevalent of the fibril-forming collagens (Kadler *et al.*, 2007). According to previous studies, we know that SPCP promoted the secretion of collagen in CCD-986sk cells. In this study, we determined the expression level of type I collagen in

granulation tissue of C57BL/6 mice. The results showed that the expression level of type I collagen was induced by SPCP in C57BL/6 mice.

In summary, after SPCP treatment, wound healing was enhanced in C57BL/6 mice. This indicated that SPCP can effectively promote wound healing. In this process, ERK, Akt and TGF-β1 signaling pathway play an important role. The results obtained in this study provide important evidence of SPCP promoting skin wound healing in C57BL/6 mice. And the mechanism was revealed. Further, the results obtained in this study can support the positive role of SPCP in wound healing.

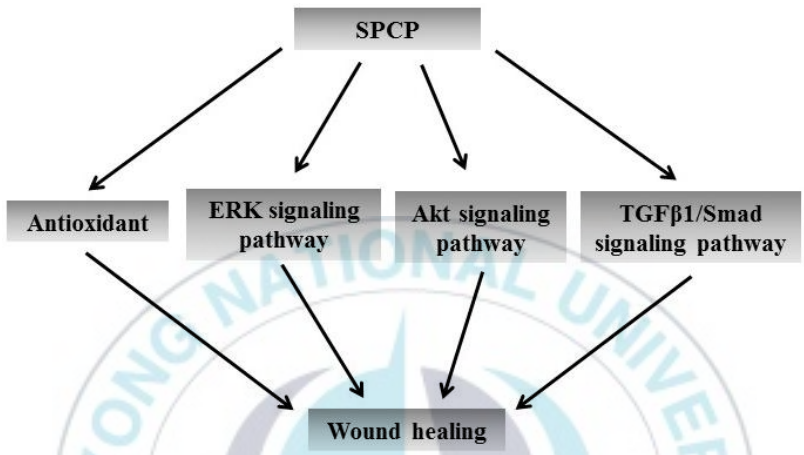

Figure 39. Effect of SPCP on the skin wound healing in C57BL/6 mice.

IV. CONCLUSION

In conclusion, in the present study, we demonstrated that the SPCP promoted the proliferation and migration of human dermal fibroblasts CCD-986sk cells. The EGFR/ERK signaling pathway and PI3K/Akt signaling pathway were activated in this process. From in vivo assay, we can see that SPCP enhanced the skin wound healing in C57BL/6 mice via ERK, Akt, and TGF-β1 signaling pathways. The results of this study provide important evidence for the potential of SPCP in promoting wound healing and reveal its mechanism in this process. Meanwhile, these results provide a potential application of SPCP in skin wound healing.

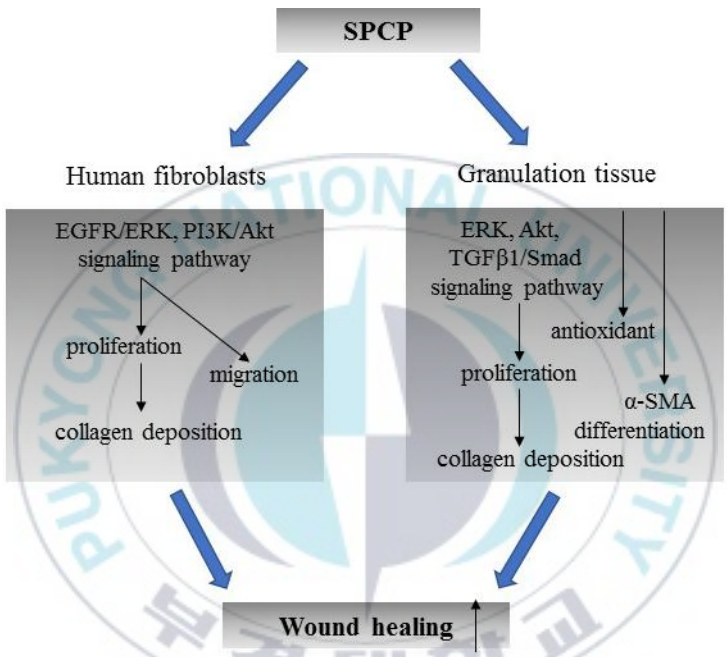

Figure 40. Graphical schematic the regulatory mechanism of SPCP in enhancing wound healing.

V. REFERENCES

Abood, W. N., Al-Henhena, N. A., Najim, A. A., Al-Obaidi, M. M., Ismail, S., Abdulla, M., and Al, B. R. (2014). Wound-healing potential of the fruit extract of Phaleria macrocarpa. *Bosn J Basic Med Sci*, 15, 25-30.

Al-Mulla, F., Leibovich, S. J., Francis, I. M., and Bitar, M. S. (2011). Impaired TGF-β signaling and a defect in resolution of inflammation contribute to delayed wound healing in a female rat model of type 2 diabetes. *Mol Biosyst*, 7, 3006-3020.

Alberola-Ila, J., and Hern ández-Hoyos, G. (2003). The Ras/MAPK cascade and the control of positive selection. *Immunol Rev*, 191, 79-96.

Ashcroft, G. S., Lei, K., Jin, W., Longenecker, G., Kulkarni, A. B., Greenwell-Wild, T., Hale-Donze, H., McGrady, G., Song, X. Y., and Wahl, S. M. (2000). Secretory leukocyte protease inhibitor mediates non-redundant functions necessary for normal wound healing. *Nat Med*, 6, 1147-1153.

Bachstetter, A. D., Jennifer, J., Andrea, S., Vila, J. L., Charles, H., Cole, M. J., R Douglas, S., Jun, T., Sanberg, P. R., and Sanberg, C. D. (2010). Spirulina promotes stem cell genesis and protects against LPS induced declines in neural stem cell proliferation. *PLoS One*, 5, e10496.

Baker, N. E. (2001). Cell proliferation, survival, and death in the Drosophila eye. *Semin Cell Dev Biol*, 12, 499-507.

Bari, E., Arciola, C. R., Vigani, B., Crivelli, B., Moro, P., Marrubini, G., Sorrenti, M., Catenacci, L., Bruni, G., and Chlapanidas, T. (2017). In vitro

effectiveness of microspheres based on silk sericin and chlorella vulgaris or arthrospira platensis for wound healing applications. *Materials*, 10, 983.

Barrientos, S., Stojadinovic, O., Golinko, M. S., Brem, H., and Tomic-Canic, M. (2008). Perspective article: Growth factors and cytokines in wound healing. *Wound Repair Regen*, 16, 585-601.

Bashandy, S. A. E., El Awdan, S. A., Ebaid, H., and Alhazza, I. M. (2016). Antioxidant potential of spirulina platensis mitigates oxidative stress and reprotoxicity induced by sodium arsenite in male rats. *Oxid Med Cell Longev*, 2016, 8.

Becker, E. W. (2007). Micro-algae as a source of protein. *Biotechnol Adv*, 25, 207-210.

Belay, A., Kato, T., and Ota, Y. (1996). Spirulina (Arthrospira): potential application as an animal feed supplement. *J Appl Phycol*, 8, 303-311.

Bertoli, C., Skotheim, J. M., and de Bruin, R. A. M. (2013). Control of cell cycle transcription during G1 and S phases. *Nat Rev Mol Cell Biol*, 14, 518-528.

Besson, A., Dowdy, S. F., and Roberts, J. M. (2008). CDK inhibitors: Cell cycle regulators and beyond. *Dev Cell*, 14, 159-169.

Bilal, M., Rasheed, T., Ahmed, I., and Hmn, I. (2017). High-value compounds from microalgae with industrial exploitability - A review. *Front Biosci*, 9, 319-342.

Bochaton-Piallat, M. L., Gabbiani, G., and Hinz, B. (2016). The myofibroblast in wound healing and fibrosis: answered and unanswered questions. *F1000Res*, 5, F1000 Faculty Rev-1752.

Boriack-Sjodin, P. A., Margarit, S. M., Bar-Sagi, D., and Kuriyan, J. (1998). The structural basis of the activation of Ras by Sos. *Nature*, 394, 337-343.

Brown, M. R., Jeffrey, S. W., Volkman, J. K., and Dunstan, G. A. (1997). Nutritional properties of microalgae for mariculture. *Aquaculture*, 151, 315-331.

Buono, S., Langellotti, A. L., Martello, A., Rinna, F., and Fogliano, V. (2014). Functional ingredients from microalgae. *Food Funct*, 5, 1669-1685.

Butch, E. R., and Guan, K. L. (1996). Characterization of ERK1 activation site mutants and the effect on recognition by MEK1 and MEK2. *J Biol Chem*, 271, 4230-4235.

Chai, X., Sun, D., Han, Q., Yi, L., Wu, Y., and Liu, X. (2018). Hypoxia induces pulmonary arterial fibroblast proliferation, migration, differentiation and vascular remodeling via the PI3K/Akt/p70S6K signaling pathway. *Int J Mol Med*, 41, 2461-2472.

Chambard, J. C., Lefloch, R., Pouysségur, J., and Lenormand, P. (2007). ERK implication in cell cycle regulation. *Biochim Biophys Acta*, 1773, 1299-1310.

Chan, T. O., and Tsichlis, P. N. (2001). PDK2: A Complex tail in one Akt. *Sci STKE*, 2001, pe1.

Chang, F., Lee, J. T., Navolanic, P. M., Steelman, L. S., Shelton, J. G., Blalock, W. L., Franklin, R. A., McCubrey, J. A. (2003). Involvement of PI3K/Akt pathway in cell cycle progression, apoptosis, and neoplastic transformation: a target for cancer chemotherapy. *Leukemia*, 17, 590-603.

Chen, H., Li, D., Saldeen, T., and Mehta, J. L. (2003). TGF-β1 attenuates myocardial ischemia-reperfusion injury via inhibition of upregulation of MMP-1. *Am J Physiol Heart Circ Physiol*, 284, H1612-H1617.

Chew, K. W., Yap, J. Y., Show, P. L., Suan, N. H., Juan, J. C., Ling, T. C., Lee, D. J., and Chang, J. S. (2017). Microalgae biorefinery: High value products perspectives. *Bioresour Technol*, 229, 53-62.

Chiloeches, A., Mason, C. S., and Marais, R. (2001). S338 phosphorylation of Raf-1 is independent of phosphatidylinositol 3-kinase and Pak3. *Mol Cell Biol*, 21, 2423-2434.

Chin, D., Boyle, G. M., Parsons, P. G., and Coman, W. B. (2004). What is transforming growth factor-beta (TGF-β)? *Int J Biochem Cell Biol*, 57, 215-221.

Chiquet, M., Katsaros, C., and Kletsas, D. (2015). Multiple functions of gingival and mucoperiosteal fibroblasts in oral wound healing and repair. *Periodontol 2000*, 68, 21-40.

Cho, K. J., Kasai, R. S., Park, J. H., Chigurupati, S., Heidorn, S. J., van der Hoeven, D., Plowman, S. J., Kusumi, A., Marais, R., and Hancock, J. F. (2012). Raf inhibitors target Ras spatiotemporal dynamics. *Curr Biol*, 22, 945-955.

Coqueret, O. (2003). New roles for p21 and p27 cell-cycle inhibitors: a function for each cell compartment? *Trends Cell Biol*, 13, 65-70.

Corcoran, R. B., Ebi, H., Turke, A. B., Coffee, E. M., Nishino, M., Cogdill, A. P., Brown, R. D., Della, P. P., Diassantagata, D., and Hung, K. E. (2012). EGFR-mediated re-activation of MAPK signaling contributes to insensitivity of BRAF mutant colorectal cancers to RAF inhibition with vemurafenib. *Cancer Discov*, 2, 227-235.

Coutant, A., Rescan, C., Gilot, D., Loyer, P., Guguen-Guillouzo, C., and Baffet, G. (2002). PI3K-FRAP/mTOR pathway is critical for hepatocyte

proliferation whereas MEK/ERK supports both proliferation and survival. *Hepatology*, 36, 1079-1088.

Crews, C., Alessandrini, A., and Erikson, R. (1992). The primary structure of MEK, a protein kinase that phosphorylates the ERK gene product. *Science*, 258, 478-480.

Crowe, M. J., Doetschman, T., and Greenhalgh, D. G. (2000). Delayed wound healing in immunodeficient TGF-β1 knockout Mice. *J Invest Dermatol*, 115, 3-11.

Cruz, C. D., and Cruz, F. (2007). The ERK 1 and 2 pathway in the nervous system: from basic aspects to possible clinical applications in pain and visceral dysfunction. *Curr Neuropharmacol*, 5, 244-252.

D'Ambrosio, S. M., Han, C., Pan, L., Douglas Kinghorn, A., and Ding, H. (2011). Aliphatic acetogenin constituents of avocado fruits inhibit human oral cancer cell proliferation by targeting the EGFR/RAS/RAF/MEK/ERK1/2 pathway. *Biochem Biophys Res Commun*, 409, 465-469.

Darby, I. A., and Hewitson, T. D. (2007). Fibroblast differentiation in wound healing and fibrosis. *Int Rev Cytol*, 257, 143-179.

Darby, I. A., Laverdet, B., Bonté, F., and Desmoulière, A. (2014). Fibroblasts and myofibroblasts in wound healing. *Clin Cosmet Investig Dermatol*, 7, 301-311.

Desmoulière, A. (1995). Factors influencing myofibroblast differentiation during wound healing and fibrosis. *Cell Biol Int*, 19, 471-476.

Desmoulière, A., Chaponnier, C., and Gabbiani, G. (2005). Perspective article: Tissue repair, contraction, and the myofibroblast. *Wound Repair Regen*, 13, 7-12.

Dhillon, A. S., and Kolch, W. (2002). Untying the regulation of the Raf-1 kinase. *Arch Biochem Biophys*, 404, 3-9.

Duronio, R. J., and Yue, X. (2013). Signaling pathways that control cell proliferation. *Cold Spring Harb Perspect Biol*, 5, a008904.

Tracy, L. E., Minasian, R. A., Caterson, E. J. (2016). Extracellular matrix and dermal fibroblast function in the healing wound. *Adv Wound Care (New Rochelle)*, 5, 119-136.

El-Tantawy, W. H. (2016). Antioxidant effects of Spirulina supplement against lead acetate-induced hepatic injury in rats. *J Tradit Complement Med*, 6, 327-331.

Engelman, J. A., Luo, J., and Cantley, L. C. (2006). The evolution of phosphatidylinositol 3-kinases as regulators of growth and metabolism. *Nat Rev Genet*, 7, 606-619.

Fetics, S. K., Guterres, H., Kearney, B. M., Buhrman, G., Ma, B., Nussinov, R., and Mattos, C. (2015). Allosteric effects of the oncogenic RasQ61L mutant on Raf-RBD. *Structure*, 23, 505-516.

Fingar, D. C., Richardson, C. J., Tee, A. R., Cheatham, L., Tsou, C., and Blenis, J. (2004). mTOR controls cell cycle progression through its cell growth effectors S6K1 and 4E-BP1/Eukaryotic translation initiation factor 4E. *Mol Cell Biol*, 24, 200-216.

Gabbiani, G. (2003). The myofibroblast in wound healing and fibrocontractive diseases. *J Pathol*, 200, 500-503.

Gao, X., Neufeld, T. P., and Pan, D. (2000). Drosophila PTEN regulates cell growth and proliferation through PI3K-dependent and -independent pathways. *Dev Biol*, 221, 404-418.

Ghosh, D., McGrail, D. J., and Dawson, M. R. (2017). TGF-β1 Pretreatment improves the function of mesenchymal stem cells in the wound bed. *Front Cell Dev Biol*, 5, 28.

Gonzalez, A. C., Costa, T. F., Andrade, Z. A., and Medrado, A. R. (2016). Wound healing - A literature review. *An Bras Dermatol*, 91, 614-620.

Grimes, C. A., and Jope, R. S. (2001). The multifaceted roles of glycogen synthase kinase 3β in cellular signaling. *Prog Neurobiol*, 65, 391-426.

Gunes, S., Tamburaci, S., Dalay, M. C., and Gurhan, I. D. (2017). In vitro evaluation of Spirulina platensis extract incorporated skin cream with its wound healing and antioxidant activities. *Pharm Biol*, 55, 1824-1832.

Guo, S., and DiPietro, L. A. (2010). Factors affecting wound healing. *J Dent Res*, 89, 219-229.

Han, M. W., Ryu, I. S., Lee, J. C., Kim, S. H., Chang, H. W., Lee, Y. S., Lee, S., Kim, S. W., and Kim, S. Y. (2018). Phosphorylation of PI3K regulatory subunit p85 contributes to resistance against PI3K inhibitors in radioresistant head and neck cancer. *Oral Oncol*, 78, 56-63.

He, Z., Jiang, J., Kokkinaki, M., Golestaneh, N., Hofmann, M. C., and Dym, M. (2008). Gdnf upregulates c-Fos transcription via the Ras/Erk1/2 pathway to promote mouse spermatogonial stem cell proliferation. *Stem Cells*, 26, 266-278.

Herbst, R. S. (2004). Review of epidermal growth factor receptor biology. *Int J Radiat Oncol Biol Phys*, 59, S21-S26.

Herman, M. P., Sukhova, G. K., Libby, P., Gerdes, N., Tang, N., Horton, D. B., Kilbride, M., Breitbart, R. E., Chun, M., and Schönbeck, U. (2001). Expression of neutrophil collagenase (matrix metalloproteinase-8) in

human atheroma: a novel collagenolytic pathway suggested by transcriptional profiling. *Circulation*, 104, 1899-1904.

Heussner, A. H., Mazija, L., Fastner, J., and Dietrich, D. R. (2012). Toxin content and cytotoxicity of algal dietary supplements. *Toxicol Appl Pharmacol*, 265, 263-271.

Hindley, A., and Kolch, W. (2002). Extracellular signal regulated kinase (ERK)/mitogen activated protein kinase (MAPK)-independent functions of Raf kinases. *J Cell Sci*, 115, 1575-1581.

Hinz, B. (2007). Formation and function of the myofibroblast during tissue repair. *J Invest Dermatol*, 127, 526-537.

Hinz, B. (2016). The role of myofibroblasts in wound healing. *Curr Res Transl Med*, 64, 171-177.

Hinz, B., Phan, S. H., Thannickal, V. J., Galli, A., Bochaton-Piallat, M. L., and Gabbiani, G. (2007). The myofibroblast: One function, multiple origins. *Am J Pathol*, 170, 1807-1816.

Hongxue, S., Yi, C., Jingjing, Y., Pingtao, C., Jinjing, Z., Rui, L., Ying, Y., Zhouguang, W., Hongyu, Z., and Cai, L. (2015). bFGF promotes the migration of human dermal fibroblasts under diabetic conditions through reactive oxygen species production via the PI3K/Akt-Rac1-JNK pathways. *Int J Biol Sci*, 11, 845-859.

Hoseini, S. M., Kalantari, A., Afarideh, M., Noshad, S., Behdadnia, A., Nakhjavani, M., and Esteghamati, A. (2015). Evaluation of plasma MMP-8, MMP-9 and TIMP-1 identifies candidate cardiometabolic risk marker in metabolic syndrome: results from double-blinded nested case-control study. *Metabolism*, 64, 527-538.

Howe, A. K., Aplin, A. E., and Juliano, R. L. (2002). Anchorage-dependent ERK signaling – mechanisms and consequences. *Curr Opin Genet Dev*, 12, 30-35.

Hu, L., Wang, J., Zhou, X., Xiong, Z., Zhao, J., Yu, R., Huang, F., Zhang, H., and Chen, L. (2016). Exosomes derived from human adipose mensenchymal stem cells accelerates cutaneous wound healing via optimizing the characteristics of fibroblasts. *Sci Rep*, 6, 32993.

Jaffer, Z. M., and Chernoff, J. (2002). p21-Activated kinases: three more join the Pak. *Int J Biochem Cell Biol*, 34, 713-717.

Janku, F., Yap, T. A., and Meric-Bernstam, F. (2018). Targeting the PI3K pathway in cancer: are we making headway? *Nat Rev Clin Oncol*, 15, 273-291.

Jeon, Y. K., Jang, Y. H., Yoo, D. R., Kim, S. N., Lee, S. K., and Nam, M. J. (2010). Mesenchymal stem cells' interaction with skin: Wound-healing effect on fibroblast cells and skin tissue. *Wound Repair Regen*, 18, 655-661.

Jester, J. V., Petroll, W. M., and Cavanagh, H. D. (1999). Corneal stromal wound healing in refractive surgery: the role of myofibroblasts. *Prog Retin Eye Res*, 18, 311-356.

Jin, Y., Ha, N., Forés, M., Xiang, J., Gläßer, C., Maldera, J., Jiménez, G., and Edgar, B. A. (2015). EGFR/Ras signaling controls drosophila intestinal stem cell proliferation via capicua-regulated genes. *PLOS Genet*, 11, e1005634.

Johnson, D. E. (2008). Src family kinases and the MEK/ERK pathway in the regulation of myeloid differentiation and myeloid leukemogenesis. *Adv Enzyme Regul*, 48, 98-112.

Johnson, G. L., and Lapadat, R. (2002). Mitogen-activated protein kinase pathways mediated by ERK, JNK, and p38 protein kinases. *Science*, 298, 1911-1912.

Jorissen, R. N., Walker, F., Pouliot, N., Garrett, T. P. J., Ward, C. W., and Burgess, A. W. (2003). Epidermal growth factor receptor: mechanisms of activation and signalling. *Exp Cell Res*, 284, 31-53.

Joshi, A., Joshi, V. K., Pandey, D., and Hemalatha, S. (2016). Systematic investigation of ethanolic extract from Leea macrophylla : Implications in wound healing. *J Ethnopharmacol*, 191, 95-106.

Jung, S. M., Kim, D. S., Ju, J. H., Shin, H. S. (2013). Assessment of Spirulina-PCL nanofiber for the regeneration of dermal fibroblast layers. *In Vitro Cell Dev Biol Anim*, 49, 27-33.

Jutten, B., and Rouschop, K. (2014). EGFR signaling and autophagy dependence for growth, survival, and therapy resistance. *Cell Cycle*, 13, 42-51.

Kadler, K. E., Baldock, C., Bella, J., and Boot-Handford, R. P. (2007). Collagens at a glance. *J Cell Sci*, 120, 1955-1958.

Kawatani, M., Fukushima, Y., Kondoh, Y., Honda, K., Sekine, T., Yamaguchi, Y., Taniguchi, N., and Osada, H. (2015). Identification of matrix metalloproteinase inhibitors by chemical arrays. *Biosci Biotechnol Biochem*, 79, 1597-1602.

Kepekçi, R. A., Polat, S., Çelik, A., Bayat, N., and Saygideger, S. D. (2013). Protective effect of Spirulina platensis enriched in phenolic compounds against hepatotoxicity induced by CCl4. *Food Chem*, 141, 1972-1979.

Kim, H. S., Sun, X., Lee, J. H., Kim, H. W., Fu, X., and Leong, K. W. (2018). Advanced drug delivery systems and artificial skin grafts for skin wound healing. *Adv Drug Deliv Rev*.

Kim, M. Y., Cheong, S. H., Lee, J. H., Kim, M. J., Sok, D. E., and Kim, M. R. (2010). Spirulina improves antioxidant status by reducing oxidative stress in rabbits fed a high-cholesterol diet. *J Med Food*, 13, 420-426.

Kim, W. S., Park, B. S., Sung, J. H., Yang, J. M., Park, S. B., Kwak, S. J., and Park, J. S. (2007). Wound healing effect of adipose-derived stem cells: A critical role of secretory factors on human dermal fibroblasts. *J Dermatol Sci*, 48, 15-24.

Knittel, T., Mehde, M., Kobold, D., Saile, B., Dinter, C., and Ramadori, G. (1999). Expression patterns of matrix metalloproteinases and their inhibitors in parenchymal and non-parenchymal cells of rat liver: regulation by TNF-α and TGF-β1. *J Hepatol*, 30, 48-60.

Kolch, W. (2000). Meaningful relationships: the regulation of the Ras/Raf/MEK/ERK pathway by protein interactions. *Biochem J*, 351, 289-305.

Komposch, K., and Sibilia, M. (2015). EGFR signaling in liver diseases. *Int J Mol Sci*, 17, 30.

Kornasio, R., Riederer, I., Butler-Browne, G., Mouly, V., Uni, Z., and Halevy, O. (2009). β-hydroxy-β-methylbutyrate (HMB) stimulates myogenic cell proliferation, differentiation and survival via the MAPK/ERK and PI3K/Akt pathways. *Biochim Biophys Acta*, 1793, 755-763.

Krasinskas, A. M. (2011). EGFR signaling in colorectal carcinoma. *Patholog Res Int*, 2011, 932932.

Kubatka, P., Kapinová, A., Kružliak, P., Kello, M., Výbohová, D., Kajo, K., Novák, M., Chripková, M., Adamkov, M., Péč, M., Mojžiš, J., Bojková, B., Kassayová, M., Stollárová, N., Dobrota, D. (2015). Antineoplastic effects

of Chlorella pyrenoidosa in the breast cancer model. *Nutrition*, 31, 560-569.

Kuo, Y. R., Wu, W. S., Jeng, S. F., Wang, F. S., Huang, H. C., Lin, C. Z., and Yang, K. D. (2005). Suppressed TGF-β1 expression is correlated with up-regulation of matrix metalloproteinase-13 in keloid regression after flashlamp pulsed-dye laser treatment. *Lasers Surg Med*, 36, 38-42.

Kurahashi, T., and Fujii, J. (2015). Roles of antioxidative enzymes in wound healing. *J Dev Biol*, 3, 57-70.

Kuriyama, M., Harada, N., Kuroda, S., Yamamoto, T., Nakafuku, M., Iwamatsu, A., Yamamoto, D., Prasad, R., Croce, C., Canaani, E., Kaibuchi, K. (1996). Identification of AF-6 and Canoe as putative targets for Ras. *J Biol Chem*, 271, 607-610.

Lai, S., and Pelech, S. (2016). Regulatory roles of conserved phosphorylation sites in the activation T-loop of the MAP kinase ERK1. *Mol Biol Cell*, 27, 1040-1050.

Landén, N. X., Li, D., and Ståhle, M. (2016). Transition from inflammation to proliferation: a critical step during wound healing. *Cell Mol Life Sci*, 73, 3861-3885.

Laplante, M., and Sabatini, D. M. (2009). mTOR signaling at a glance. *J Cell Sci*, 122, 3589-3594.

Laplante, M., and Sabatini, D. M. (2012). mTOR signaling in growth control and disease. *Cell*, 149, 274-293.

Lawrence, J. C., and Abraham, R. T. (1997). PHAS/4E-BPs as regulators of mRNA translation and cell proliferation. *Trends Biochem Sci*, 22, 345-349.

Lee, J., Park, A., Kim, M. J., Lim, H. J., Rha, Y. A., and Kang, H. G. (2017). Spirulina extract enhanced a protective effect in type 1 diabetes by anti-apoptosis and anti-ROS production. *Nutrients*, 9, 1363.

Lee, J. J., Loh, K., and Yap, Y. S. (2015). PI3K/Akt/mTOR inhibitors in breast cancer. *Cancer Biol Med*, 12, 342-354.

Li-Chen, W., Ja-An Annie, H., Ming-Chen, S., and In-Wei, L. (2005). Antioxidant and antiproliferative activities of Spirulina and Chlorella water extracts. *J Agric Food Chem*, 53, 4207.

Li, B., Qiu, T., Zhang, P., Wang, X., Yin, Y., and Li, S. (2014). IKVAV regulates ERK1/2 and Akt signalling pathways in BMMSC population growth and proliferation. *Cell Prolif*, 47, 133-145.

Li, B., and Wang, J. H. (2011). Fibroblasts and myofibroblasts in wound healing: Force generation and measurement. *J Tissue Viability*, 20, 108-120.

Li, Z., Liu, S., and Cai, Y. (2015). EGFR/MAPK signaling regulates the proliferation of drosophila renal and nephric stem cells. *J Genet Genomics*, 42, 9-20.

Liang, S. I., van Lengerich, B., Eichel, K., Cha, M., Patterson, D. M., Yoon, T. Y., von Zastrow, M., Jura, N., and Gartner, Z. J. (2018). Phosphorylated EGFR dimers are not sufficient to activate Ras. *Cell Rep*, 22, 2593-2600.

Lichtman, M. K., Otero-Vinas, M., and Falanga, V. (2016). Transforming growth factor beta (TGF-β) isoforms in wound healing and fibrosis. *Wound Repair Regen*, 24, 215-222.

Ling, L., Wei, T., He, L., Wang, Y., Wang, Y., Feng, X., Zhang, W., and Xiong, Z. (2017). Low-intensity pulsed ultrasound activates ERK1/2 and PI3K-Akt signalling pathways and promotes the proliferation of human amnion-derived mesenchymal stem cells. *Cell Prolif*, 50.

Liu, C., Li, Y., Semenov, M., Han, C., Baeg, G. H., Tan, Y., Zhang, Z., Lin, X., and He, X. (2002). Control of β-Catenin phosphorylation/degradation by a dual-kinase mechanism. *Cell*, 108, 837-847.

Liu, S., Gao, F., Wen, L., Ouyang, M., Wang, Y., Wang, Q., Luo, L., and Jian, Z. (2017). Osteocalcin induces proliferation via positive activation of the PI3K/Akt, P38 MAPK pathways and promotes differentiation through activation of the GPRC6A-ERK1/2 pathway in C2C12 myoblast cells. *Cell Physiol Biochem*, 43, 1100-1112.

Mac Neil, S. (1994). What role does the extracellular matrix serve in skin grafting and wound healing? *Burns*, 20, S67-S70.

Madhyastha, H., Madhyastha, R., Nakajima, Y., Omura, S., and Maruyama, M. (2012). Regulation of growth factors-associated cell migration by C-phycocyanin scaffold in dermal wound healing. *Clin Exp Pharmacol Physiol*, 39, 13-19.

Maehama, T., and Dixon, J. E. (1999). PTEN: a tumour suppressor that functions as a phospholipid phosphatase. *Trends Cell Biol*, 9, 125-128.

Makoto, T., Wendy, L., and Mayumi, I. (2015). Wound healing and skin regeneration. *Cold Spring Harb Perspect Med*, 5, a023267.

Manikarna, D., Uma, D., Namrata, S., Debasish, B., and Parimal, K. (2015). PI3K-mediated proliferation of fibroblasts by calendula officinalis tincture: implication in wound healing. *Phytother Res*, 29, 607-616.

Margarit, S. M., Sondermann, H., Hall, B. E., Nagar, B., Hoelz, A., Pirruccello, M., Bar-Sagi, D., and Kuriyan, J. (2003). Structural evidence for feedback activation by Ras·GTP of the Ras-specific nucleotide exchange factor SOS. *Cell*, 112, 685-695.

Martin, P. (1997). Wound healing--aiming for perfect skin regeneration. *Science*, 276, 75-81.

Martinez-Lopez, N., and Singh, R. (2014). ATGs: Scaffolds for MAPK/ERK signaling. *Autophagy*, 10, 535-537.

McAnulty, R. J. (2007). Fibroblasts and myofibroblasts: Their source, function and role in disease. *Int J Biochem Cell Biol*, 39, 666-671.

McCubrey, J. A., Steelman, L. S., Chappell, W. H., Abrams, S. L., Wong, E. W., Chang, F., Lehmann, B., Terrian, D. M., Milella, M., Tafuri, A., Stivala, F., Libra, M., Basecke, J., Evangelisti, C., Martelli, A. M., Franklin, R. A. (2007). Roles of the Raf/MEK/ERK pathway in cell growth, malignant transformation and drug resistance. *Biochim Biophys Acta*, 1773, 1263-1284.

Mebratu, Y., and Tesfaigzi, Y. (2009). How ERK1/2 activation controls cell proliferation and cell death: Is subcellular localization the answer? *Cell Cycle*, 8, 1168-1175.

Meinke, M. C., Nowbary, C. K., Schanzer, S., Vollert, H., Lademann, J., and Darvin, M. E. (2017). Influences of orally taken carotenoid-rich curly kale extract on collagen I/elastin index of the skin. *Nutrients*, 9, 775.

Meloche, S., and Pouysségur, J. (2007). The ERK1/2 mitogen-activated protein kinase pathway as a master regulator of the G1- to S-phase transition. *Oncogene*, 26, 3227-3239.

Mercado-Pimentel, M. E., Igarashi, S., Dunn, A. M., Behbahani, M., Miller, C., Read, C. M., and Jacob, A. (2016). The novel small molecule inhibitor, OSU-T315, suppresses vestibular schwannoma and meningioma growth by

inhibiting PDK2 function in the AKT pathway activation. *Austin J Med Oncol*, 3, 1025.

Milella, M., Falcone, I., Conciatori, F., Cesta Incani, U., Del Curatolo, A., Inzerilli, N., Nuzzo, C. M., Vaccaro, V., Vari, S., Cognetti, F., Ciuffreda, L. (2015). PTEN: Multiple functions in human malignant tumors. *Front Oncol*, 5, 24.

Mitra, A., Raychaudhuri, S. K., and Raychaudhuri, S. P. (2012). IL-22 induced cell proliferation is regulated by PI3K/Akt/mTOR signaling cascade. *Cytokine*, 60, 38-42.

Mukohara, T. (2015). PI3K mutations in breast cancer: prognostic and therapeutic implications. *Breast cancer (Dove Med Press)*, 7, 111-123.

Nimse, S. B., and Pal, D. (2015). Free radicals, natural antioxidants, and their reaction mechanisms. *RSC Adv*, 5, 27986-28006.

Nusse, R., and Clevers, H. (2017). Wnt/β-Catenin signaling, disease, and emerging therapeutic modalities. *Cell*, 169, 985-999.

Okizaki, S., Ito, Y., Hosono, K., Oba, K., Ohkubo, H., Amano, H., Shichiri, M., and Majima, M. (2015). Suppressed recruitment of alternatively activated macrophages reduces TGF-β1 and impairs wound healing in streptozotocin-induced diabetic mice. *Biomed Pharmacother*, 70, 317-325.

Park, H. H., Park, N. Y., Kim, S. G., Jeong, K. T., Lee, E. J., and Lee, E. (2015). Potential wound healing activities of galla rhois in human fibroblasts and keratinocytes. *Am J Chin Med*, 43, 1625-1636.

Park, S. Y., Lee, Y. K., Lee, W. S., Park, O. J., and Kim, Y. M. (2014). The involvement of AMPK/GSK3-beta signals in the control of metastasis and proliferation in hepato-carcinoma cells treated with anthocyanins

extracted from Korea wild berry Meoru. *BMC Complement Altern Med*, 14, 109.

Patil, J., Matte, A., Mallard, C., and Sandberg, M. (2018). Spirulina diet to lactating mothers protects the antioxidant system and reduces inflammation in post-natal brain after systemic inflammation. *Nutr Neurosci*, 21, 59-69.

Peng, S., Zhang, Y., Zhang, J., Wang, H., and Ren, B. (2010). ERK in learning and memory: A review of recent research. *Int J Mol Sci*, 11, 222-232.

Pereira, R. F., Bártolo, P. J. (2016). Traditional therapies for skin wound healing. *Adv Wound Care (New Rochelle)*, 5, 208-229.

Plikus, M. V., Guerrero-Juarez, C. F., Ito, M., Li, Y. R., Dedhia, P. H., Zheng, Y., Shao, M., Gay, D. L., Ramos, R., Hsi, T. C., Oh, J. W., Wang, X., Ramirez, A., Konopelski, S. E., Elzein, A., Wang, A., Supapannachart, R. J., Lee, H. L., Lim, C. H., Nace, A., Guo, A., Treffeisen, E., Andl, T., Ramirez, R. N., Murad, R., Offermanns, S., Metzger, D., Chambon, P., Widgerow, A. D., Tuan, T. L., Mortazavi, A., Gupta, R. K., Hamilton, B. A., Millar, S. E., Seale, P., Pear, W. S., Lazar, M. A., Cotsarelis, G. (2017). Regeneration of fat cells from myofibroblasts during wound healing. *Science*, 355, 748-752.

Ponnusamy, M., Li, P. F., and Wang, K. (2017). Understanding cardiomyocyte proliferation: an insight into cell cycle activity. *Cell Mol Life Sci*, 74, 1019-1034.

Puolakkainen, P. A., Twardzik, D. R., Ranchalis, J. E., Pankey, S. C., Reed, M. J., and Gombotz, W. R. (1995). The Enhancement in wound healing by transforming growth factor-β1 (TGF-β1) depends on the topical delivery system. *J Sur Res*, 58, 321-329.

Rajaram, P., Chandra, P., Ticku, S., Pallavi, B., Rudresh, K., and Mansabdar, P. (2017). Epidermal growth factor receptor: Role in human cancer. *Indian J Dent Res*, 28, 687-694.

Ram, M., Singh, V., Kumar, D., Kumawat, S., Gopalakrishnan, A., Lingaraju, M. C., Gupta, P., Tandan, S. K., and Kumar, D. (2014). Antioxidant potential of bilirubin-accelerated wound healing in streptozotocin-induced diabetic rats. *Naunyn Schmiedebergs Arch Pharmacol*, 387, 955-961.

Raposo, M. F. D. J., and Rui, M. S. C. D. M. (2013). Health applications of bioactive compounds from marine microalgae. *Life Sci*, 93, 479-486.

Roberts, P. J., and Der, C. J. (2007). Targeting the Raf-MEK-ERK mitogen-activated protein kinase cascade for the treatment of cancer. *Oncogene*, 26, 3291-3310.

Rojas, M., Yao, S., and Lin, Y. Z. (1996). Controlling epidermal growth factor (EGF)-stimulated Ras activation in intact cells by a cell-permeable peptide mimicking phosphorylated EGF receptor. *J Biol Chem*, 271, 27456-27461.

Rozakis-Adcock, M., Fernley, R., Wade, J., Pawson, T., and Bowtell, D. (1993). The SH2 and SH3 domains of mammalian Grb2 couple the EGF receptor to the Ras activator mSos1. *Nature*, 363, 83-85.

Ruoff, R., Katsara, O., and Kolupaeva, V. (2016). Cell type-specific control of protein synthesis and proliferation by FGF-dependent signaling to the translation repressor 4E-BP. *Proc Natl Acad Sci U S A*, 113, 7545-7550.

Sailaja Rao, P., Kalva, S., Yerramilli, A., and Mamidi, S. (2011). Free radicals and tissue damage: Role of antioxidants. *Free Radicals and Antioxidants* 1, 2-7.

Salsasescat, R., Nerenberg, P. S., and Stultz, C. M. (2010). Cleavage site specificity and conformational selection in type I collagen degradation. *Biochemistry*, 49, 4147-4158.

Sanchez, A., Blanco, M., Correa, B., Perez-Martin, R., and Sotelo, C. (2018). Effect of fish collagen hydrolysates on type I collagen mRNA levels of human dermal fibroblast culture. *Mar Drugs*, 16, 144.

Saranraj, P. (2014). Spirulina platensis-food for future: a review. *AJPST*, 1, 26-33.

Schevzov, G., Kee, A. J., Wang, B., Sequeira, V. B., Hook, J., Coombes, J. D., Lucas, C. A., Stehn, J. R., Musgrove, E. A., Cretu, A., Assoian, R., Fath, T., Hanoch, T., Seger, R., Pleines, I., Kile, B. T., Hardeman, E. C., and Gunning, P. W. (2015). Regulation of cell proliferation by ERK and signal-dependent nuclear translocation of ERK is dependent on Tm5NM1-containing actin filaments. *Mol Biol Cell*, 26, 2475-2490.

Schreier, B., Gekle, M., and Grossmann, C. (2014). Role of epidermal growth factor receptor in vascular structure and function. *Curr Opin Nephrol Hypertens*, 23, 113-121.

Schultz, G. S., and Wysocki, A. (2009). Interactions between extracellular matrix and growth factors in wound healing. *Wound Repair and Regen*, 17, 153-162.

Sears, R. C., and Nevins, J. R. (2002). Signaling networks that link cell proliferation and cell fate. *J Biol Chem*, 277, 11617-11620.

Sethi, T., Ginsberg, M. H., Downward, J., and Hughes, P. E. (1999). The small GTP-binding protein R-Ras can influence integrin activation by antagonizing a Ras/Raf-initiated integrin suppression pathway. *Mol Biol Cell*, 10, 1799-1809.

Sheaff, R. J., Groudine, M., Gordon, M., Roberts, J. M., Clurman, B. E. (1997). Cyclin E-CDK2 is a regulator of p27Kip1. *Genes Dev*, 11, 1464-1478.

Sheih, I. C., Fang, T. J., Wu, T. K., and Lin, P. H. (2010). Anticancer and antioxidant activities of the peptide fraction from algae protein waste. *J Agric Food Chem*, 58, 1202-1207.

Shoulders, M. D., and Raines, R. T. (2010). Collagen structure and stability. *Annu Rev Biochem*, 78, 929-958.

Sies, H. (2017). Hydrogen peroxide as a central redox signaling molecule in physiological oxidative stress: Oxidative eustress. *Redox Biol*, 11, 613-619.

Singer, A. J., and Clark, R. A. (1999). Cutaneous wound healing. *N Engl J Med*, 341, 738-746.

Sohn, H. Y., Keller, M., Gloe, T., Morawietz, H., Rueckschloss, U., and Pohl, U. (2000). The small G-protein rac mediates depolarization-induced superoxide formation in human endothelial cells. *J Biol Chem*, 275, 18745-18750.

Sorg, H., Tilkorn, D. J., Hager, S., Hauser, J., and Mirastschijski, U. (2017). Skin wound healing: An update on the current knowledge and concepts. *Eur Surg Res*, 58, 81-94.

Spolaore, P., Joannis-Cassan, C., Duran, E., and Isambert, A. (2006). Commercial applications of microalgae. *J Biosci Bioeng*, 101, 87-96.

Stewart, E. L., Tan, S. Z., Liu, G., and Tsao, M. S. (2015). Known and putative mechanisms of resistance to EGFR targeted therapies in NSCLC patients with EGFR mutations-a review. *Transl Lung Cancer Res*, 4, 67-81.

Sun, Y., Liu, W. Z., Liu, T., Feng, X., Yang, N., and Zhou, H. F. (2015). Signaling pathway of MAPK/ERK in cell proliferation, differentiation, migration, senescence and apoptosis. *J Recept Signal Transduct Res*, 35, 600-604.

Sun, Y. B., Qu, X., Caruana, G., and Li, J. (2016). The origin of renal fibroblasts/myofibroblasts and the signals that trigger fibrosis. *Differentiation*, 92, 102-107.

Syarina, P. N., Karthivashan, G., Abas, F., Arulselvan, P., and Fakurazi, S. (2015). Wound healing potential of Spirulina platensis extracts on human dermal fibroblast cells. *EXCLI J*, 14, 385-393.

Takino, K., Ohsawa, S., and Igaki, T. (2014). Loss of Rab5 drives non-autonomous cell proliferation through TNF and Ras signaling in Drosophila. *Dev Biol*, 395, 19-28.

Tee, A. R., and Blenis, J. (2005). mTOR, translational control and human disease. *Semin Cell Dev Biol*, 16, 29-37.

Tracy, L. E., Minasian, R. A., and Caterson, E. J. (2014). Extracellular matrix and dermal fibroblast function in the healing wound. *Adv Wound Care (New Rochelle)*, 5, 119-136.

Valenta, T., Hausmann, G., and Basler, K. (2012). The many faces and functions of β-catenin. *EMBO J*, 31, 2714-2736.

van den Heuvel, S., and Harlow, E. (1993). Distinct roles for cyclin-dependent kinases in cell cycle control. *Science*, 262, 2050-2054.

Vanhaesebroeck, B., Whitehead, M. A., and Piñeiro, R. (2016). Molecules in medicine mini-review: isoforms of PI3K in biology and disease. *J Mol Med (Berl)*, 94, 5-11.

Vara, J. Á. F., Casado, E., de Castro, J., Cejas, P., Belda-Iniesta, C., and González-Barón, M. (2004). PI3K/Akt signalling pathway and cancer. *Cancer Treat Rev*, 30, 193-204.

Verrecchia, F., and Mauviel, A. (2002). Transforming growth factor-β signaling through the smad pathway: Role in extracellular matrix gene expression and regulation. *J Invest Dermatol*, 118, 211-215.

Vojtek, A. B., and Der, C. J. (1998). Increasing complexity of the Ras signaling pathway. *J Biol Chem*, 273, 19925-19928.

Wang, F. P., Li, L., Li, J., Wang, J. Y., Wang, L. Y., and Jiang, W. (2013). High mobility group box-1 promotes the proliferation and migration of hepatic stellate cells via TLR4-dependent signal pathways of PI3K/Akt and JNK. *PLoS One*, 8, e64373.

Wang, Z. G., Wang, Y., Huang, Y., Lu, Q., Zheng, L., Hu, D., Feng, W. K., Liu, Y. L., Ji, K. T., Zhang, H. Y., Fu, X. B., Li, X. K., Chu, M. P., Xiao, J. (2015). bFGF regulates autophagy and ubiquitinated protein accumulation induced by myocardial ischemia/reperfusion via the activation of the PI3K/Akt/mTOR pathway. *Sci Rep*, 5, 9287.

Wang, Z., and Zhang, X. (2016). Isolation and identification of anti-proliferative peptides from Spirulina platensis using three-step hydrolysis. *J Sci Food Agric*, 97, 918-922.

Wei, Z., and Hui, T. L. (2002). MAPK signal pathways in the regulation of cell proliferation in mammalian cells. *Cell Res*, 12, 9-18.

Werner, S., Krieg, T., and Smola, H. (2007). Keratinocyte-fibroblast interactions in wound healing. *J Invest Dermatol*, 127, 998-1008.

Wiegand, C., Abel, M., Ruth, P., and Hipler, U. C. (2011). Superabsorbent polymer-containing wound dressings have a beneficial effect on wound healing by reducing PMN elastase concentration and inhibiting microbial growth. *J Mater Sci Mater Med*, 22, 2583-2590.

Woodley, D. T. (2017). Distinct fibroblasts in the papillary and reticular dermis: implications for wound healing. *Dermatol Clin*, 35, 95-100.

Wortzel, I., and Seger, R. (2011). The ERK cascade: distinct functions within various subcellular organelles. *Genes Cancer*, 2, 195-209.

Wu, H. Y., Wu, J. L., and Ni, Z. L. (2019). Overexpression of microRNA-202-3p protects against myocardial ischemia-reperfusion injury through activation of TGF-β1/Smads signaling pathway by targeting TRPM6. *Cell Cycle*, 18, 1-17.

Wu, Q., Liu, L., Miron, A., Klímová, B., Wan, D., and Kuča, K. (2016). The antioxidant, immunomodulatory, and anti-inflammatory activities of Spirulina: an overview. *Arch Toxicol*, 90, 1817-1840.

Wu, X., Li, S., Xue, P., and Li, Y. (2017). Liraglutide, a glucagon-like peptide-1 receptor agonist, facilitates osteogenic proliferation and differentiation in MC3T3-E1 cells through phosphoinositide 3-kinase (PI3K)/protein kinase B (AKT), extracellular signal-related kinase (ERK)1/2, and cAMP/protein kinase A (PKA) signaling pathways involving β-catenin. *Exp Cell Res*, 360, 281-291.

Wynn, T. A., and Vannella, K. M. (2016). Macrophages in tissue repair, regeneration, and fibrosis. *Immunity*, 44, 450-462.

Yang, Y., Xia, T., Zhi, W., Wei, L., Weng, J., Zhang, C., and Li, X. (2011). Promotion of skin regeneration in diabetic rats by electrospun core-sheath

fibers loaded with basic fibroblast growth factor. *Biomaterials*, 32, 4243-4254.

Yannas, I. V., Tzeranis, D. S., and So, P. T. (2017). Regeneration of injured skin and peripheral nerves requires control of wound contraction, not scar formation. *Wound Repair Regen*, 25, 177-191.

Young, A., Lyons, J., Miller, A. L., Phan, V. T., Alarcón, I. R., and McCormick, F. (2009). Chapter 1 Ras signaling and therapies. *Adv Cancer Res*, 102, 1-17.

Yu, J. S. L., and Cui, W. (2016). Proliferation, survival and metabolism: the role of PI3K/AKT/mTOR signalling in pluripotency and cell fate determination. *Development*, 143, 3050-3060.

Zebisch, A., and Troppmair, J. (2006). Back to the roots: the remarkable RAF oncogene story. *Cell Mol Life Sci*, 63, 1314-1330.

Zhang C. Y., Li X. H., Zhang T., Fu J., Cui X. D. (2013). Hydrogen sulfide suppresses the expression of MMP-8, MMP-13, and TIMP-1 in left ventricles of rats with cardiac volume overload. *Acta Pharmacol Sin*, 34, 1301-1309.

Zhang, L., Lee, K. C., Bhojani, M. S., Khan, A. P., Shilman, A., Holland, E. C., Ross, B. D., and Rehemtulla, A. (2007). Molecular imaging of Akt kinase activity. *Nat Med*, 13, 1114-1119.

Zhang, W., and Liu, H. T. (2002). MAPK signal pathways in the regulation of cell proliferation in mammalian cells. *Cell Res*, 12, 9-18.

Zhao, M. (2007). PTEN: a promising pharmacological target to enhance epithelial wound healing. *Br J Pharmacol*, 152, 1141-1144.

Zhao, X., Wu, H., Guo, B., Dong, R., Qiu, Y., and Ma, P. X. (2017). Antibacterial anti-oxidant electroactive injectable hydrogel as self-healing wound

dressing with hemostasis and adhesiveness for cutaneous wound healing. *Biomaterials*, 122, 34-47.

Zheng, C. F., Guan, K. L. (1994). Cytoplasmic localization of the mitogen-activated protein kinase activator MEK. *J Biol Chem*, 269, 19947-19952.

Zhong, S. P., Zhang, Y. Z., and Lim, C. T. (2010). Tissue scaffolds for skin wound healing and dermal reconstruction. *Wiley Interdiscip Rev Nanomed Nanobiotechnol*, 2, 510-525.